Contents lists available at ScienceDirect

Separation and Purification Technology

journal homepage: www.elsevier.com

Integrated photocatalytic advanced oxidation system (TiO_2/UV/O_3/H_2O_2) for degradation of volatile organic compounds

André Fernandes [a], Michał Gągol [a], Patrycja Makoś [a], Javed Ali Khan [b], Grzegorz Boczkaj [a, *]

[a] Gdansk University of Technology, Faculty of Chemistry, Department of Process Engineering and Chemical Technology, 80 – 233 Gdansk, G. Narutowicza St. 11/12, Poland
[b] Radiation Chemistry Laboratory, National Centre of Excellence in Physical Chemistry, University of Peshawar, Peshawar 25120, Pakistan

ARTICLE INFO

Keywords:
Photocatalysis
TiO_2
VOC
Wastewater treatment
Ozonation
Peroxone

ABSTRACT

Several advanced oxidation processes (AOPs) including photocatalytic processes were studied for effective treatment of complex model wastewater containing a wide variety of VOCs. The studies revealed synergistic effects of TiO_2 based processes for improved degradation of the VOCs. A peroxone combined with TiO_2/UV system (TiO_2/UV/O_3/H_2O_2) with a ratio between the oxygen source from the oxidant to chemical oxygen demand (COD) of the model wastewater (r_{ox}) of 0.5 and 100 mgTiO_2/L was the optimal process. TiO_2 revealed to be economically reasonable to be used in TiO_2/UV/H_2O_2 and TiO_2/UV/O_3/H_2O_2 photocatalytic technologies for efficient and fast (100 min) degradation of VOCs with significantly low amounts of chemicals. Developed system provide high effectiveness with low treatment cost, which in case of most VOCs studied provide satisfactory effects in 15 min. of treatment process with 4 $/m^3 of process costs. The technologies are promising in degradation and purification in several types of industrial effluents with a high VOCs content.

1. Introduction

The studies on effective methods for complete degradation of volatile organic compounds (VOCs) are very important, since, a vast variety of industrial facilities generate VOCs in their processes and in many cases they are present in the industrial effluents. Pharmaceutical [1], petroleum and refinery [2,3], paper [4,5], dye [6], tanning and textile [7], paint, gas [8], biogas [9], food [10] among others are some examples of industries which generate VOCs. Primary, the VOCs are often present in the flue gases, which are treated by absorption in aqueous media, forming effluents [11,12]. This approach allows to minimize the gas emission to the atmosphere – only non-absorbable gaseous compounds are introduced to thermal treatment (incineration). The importance of wastewater treatment regarding VOCs is related with few factors. Firstly, with the high biotoxicity of some groups of the VOCs to microorganisms, which makes ineffective the usage of biological methods to degrade such compounds. Secondly, open air treatment technologies (common practice at biological treatment stage) can increase the risk of VOCs emission to the atmosphere instead of their quantitative degradation. Thirdly and maybe one of the most important factors, the majority of the compounds present in this work are harmful to the animal and human health. Compounds like phenol [13] and di-tert-butyldisulfide are known to be toxic to aquatic and flora ecosystems and also dangerous to the human health. Dibutylsulfide [14], cresols [15] and Benzene, Toluene, Ethylbenzene, Xylene (BTEX) [16] are known to be toxic to the human health. Benzene [17] naphthalene [18] and nitro-aromatic compounds, i.e., nitrobenzene, nitrotoluene and nitrophenol [19,20] have been reported to have more harmful effects on the human health such as mutational and carcinogenic effects. Thus, such compounds must be effectively degraded by means of proper technology without formation of any toxic by-products.

Advanced oxidation processes (AOPs) have gained significant attention in the recent years for the treatment of VOCs. They were first reported by Glaze and co-workers, who stated that AOPs are capable of generating highly reactive species named hydroxyl radicals ($HO^{\bullet}$) [21]. $HO^{\bullet}$ possesses a high oxidation potential (E° = 2.7 V) and capable of oxidizing the majority of the organic pollutants [22–24]. AOPs are seen as environmental friendly technologies, since their reaction with inorganic and organic compounds can generate CO_2, H_2O and inorganic compounds in case of full mineralization [25].

Photocatalysis is one of the most studied and economically feasible AOPs. Several types of catalysts are generally applied in AOPs such as TiO_2 [26,27], ZnO [28,29], bismuth [30,31] and other complex nanos-

* Corresponding author.
Email address: grzegorz.boczkaj@pg.edu.pl (G. Boczkaj)

https://doi.org/10.1016/j.seppur.2019.05.012
Received 6 February 2019; Received in revised form 2 May 2019; Accepted 3 May 2019
Available online xxx
1383-5866/

Post-print of: Fernandes A., Gągol M., Makoś P., Khan J.A., Boczkaj G.: Integrated photocatalytic advanced oxidation system (TiO2/UV/O3/H2O2) for degradation of volatile organic compounds. SEPARATION AND PURIFICATION TECHNOLOGY. Vol. 224 (2019), pp. 1-14. DOI: https://doi.org/10.1016/j.seppur.2019.05.012

Table 1
Operational parameters and COD reduction of the processes studied.

Experiment number	Process	r_{ox}	Oxidant amount (g)	[TiO_2] (mg/L)	COD reduction (%)
1	TiO_2/UV/O_3	0.70	12	100	41
2	TiO_2/UV/O_3	0.70	12	500	44
3	TiO_2/UV/O_3	0.70	12	1000	42
4	TiO_2/UV/O_3	0.70	12	2000	43
5	TiO_2/UV/O_3	1.50	24	500	55
6	TiO_2/UV/O_3	0.4	6	500	40
7	TiO_2/UV/O_3	3.4	57.24	500	66
8	TiO_2/UV/H_2O_2	0.50	5.84	100	13
9	TiO_2/UV/H_2O_2	0.50	5.84	500	14
10	TiO_2/UV/H_2O_2	0.5	5.84	1000	13
11	TiO_2/UV/H_2O_2	1.1	11	100	18
12	TiO_2/UV/H_2O_2	0.27	2.75	100	8
13	TiO_2/UV/O_3/H_2O_2	0.50	O_3: 5.92; H_2O_2: 1.78	100	38
14	TiO_2/UV/O_3/H_2O_2	0.50	O_3: 5.92; H_2O_2: 1.78	500	33
15	TiO_2/UV/O_3/H_2O_2	0.50	O_3: 5.92; H_2O_2: 1.78	1000	37
16	TiO_2/UV/O_3/H_2O_2	0.26	O_3: 2.96; H_2O_2: 0.89	100	26
17	TiO_2/UV/O_3/H_2O_2	1.1	O_3: 11.84;H_2O_2: 3.55	100	43
18	TiO_2	–	–	100	–
19	TiO_2	–	–	500	–
20	H_2O_2	1.09	11	–	−8
21	H_2O_2/UV	1.09	11	–	−18
22	O_3	0.68	12	–	29
23	O_3/UV	0.68	12	–	43
24	O_3/H_2O_2	0.51	O_3: 5.92; H_2O_2: 1.78	–	32
25	O_3/H_2O_2/UV	0.51	O_3: 5.92; H_2O_2: 1.78	–	46

tructures [32,33]. In photocatalytic process, light photons are bombarded over a semiconductor particle (SMP), in this work titanium dioxide (TiO_2), which results in the formation of several reactive radicals which are responsible for the oxidation of organic compounds [34–41]. When irradiated with enough energy, an electron (e^-) from the valence band (VB) of SMP transfer to its conduction band (CB), leaving behind a positive hole in the CB (h_{VB}^+). The e^--h_{VB}^+ pair initiates a number of redox reactions especially the ones with the surface adsorbed water molecules which finally lead to formation of $HO^\bullet$ on the surface of TiO_2.

Literature regarding photocatalytic processes at alkaline pH revealed that its effectiveness depends upon the point of zero charge (PZC) of the catalyst used and the dissociation constant (pKa) of the compounds under study [42]. Thus, the effectiveness of the photocatalytic process using TiO_2 will always depend on the pKa of the VOCs studied.

The generality of the research of the AOPs in treating different types of VOCs mainly focuses on specific compounds, including studies of the scavengers effect on their degradation. This phenomenon strongly limits the range of application of the methods studied. In addition, real effluents contain more than one type of VOCs and their interaction may affect their degradation. These facts sustain a methodology of research on the applicational value of the developed technology for a specific type of industrial effluent. where first the technology needs to be tested using a model WW containing several VOCs, widely present in industrial effluents, and in the second step evaluated using real effluents. Some studies did such approach by testing some types of AOPs in the treatment of several types of VOCs in the same water matrix [43–47]. Thus, the aim of this work is to evaluate the performance of the photocatalytic and photolytic technologies in caustic model WW containing several VOCs to check if these technologies have the potential to be applied for highly polluted real effluents. With a proper degradation of the VOCs, there is an increase in the treatment efficiency of the biological technologies, commonly used in several types of industries, providing an important contribution for further purification of the treated effluent before being discharge to the environment.

2. Experimental

2.1. Materials

Hydrogen peroxide (30% w/v) and sodium hydroxide were purchased from POCH Poland and AEROXIDE® TiO_2 P-25 was kindly provided by EVONIK industries. The surface area given by the supplier is between 35 and 65 m^2/g and the particle size is between 2 and 3 μm.

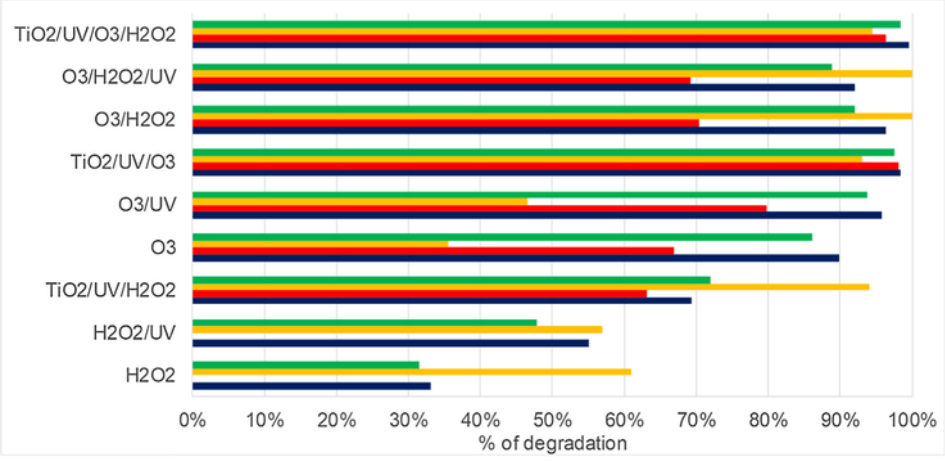

Fig. 1. Influence of the UV and photocatalytic activity in O_3, H_2O_2 and O_3/H_2O_2 processes for the degradation of the VOCs degradation. TiO_2/UV/O_3/H_2O_2 (Table 1, exp. 13); O_3/H_2O_2/UV (Table 1, exp. 25), O_3/H_2O_2 (Table 1, exp 24); TiO_2/UV/O_3 (Table 1, exp. 2); O_3/UV (Table 1, exp. 23); O_3 (Table 1, exp. 22); TiO_2/UV/H_2O_2 (Table 1, exp. 11); H_2O_2/UV (Table 1, exp. 21); H_2O_2 (Table 1, exp. 20). Green columns, total- volatile organic compounds (t-VOCs); Yellow columns, sulfur volatile organic compounds (VSCs); Red columns, nitrogen volatile organic compounds (VNCs); Blue columns, oxygen volatile organic compounds (O-VOCs). H_2O_2: VNCs degradation, −194%; t-VOCs degradation, −8%. H_2O_2/UV: VNCs degradation, −270%.

Table 2
Degradation of the studied volatile organic compounds in the different non-UV, UV and photocatalytic processes.

Compound	H_2O_2	H_2O_2/UV	TiO_2/UV/H_2O_2	O_3	O_3/UV	TiO_2/UV/O_3	O_3/H_2O_2	O_3/H_2O_2/UV	TiO_2/UV/O_3/H_2O_2
	Experiment number (according to Table 1)								
	20	21	11	22	23	2	24	25	13
Benzene	39.8%	42.8%	52.5%	96.1%	100.0%	99.5%	100.0%	100.0%	100.0%
Toluene	25.8%	51.5%	59.5%	89.7%	95.4%	99.6%	100.0%	100.0%	100.0%
ethylbenzene	12.2%	66.7%	66.2%	84.7%	91.0%	99.6%	100.0%	100.0%	100.0%
Furfural	−185.4%	66.8%	59.3%	65.2%	100.0%	88.4%	100.0%	100.0%	99.0%
o-xylene	15.3%	62.5%	60.4%	88.2%	92.6%	99.3%	100.0%	100.0%	99.5%
Phenol	35.6%	49.4%	42.4%	96.9%	98.2%	99.6%	97.8%	99.4%	99.5%
Dibutyl sulfide	42.7%	23.1%	93.7%	−26.2%	−6.3%	88.3%	100.0%	100.0%	94.6%
o-cresol	61.0%	71.2%	99.0%	78.4%	86.1%	99.7%	100.0%	100.0%	99.6%
m-cresol	46.7%	69.2%	99.3%	95.1%	100.0%	100.0%	100.0%	100.0%	100.0%
tert-butyl disulfide	100.0%	100.0%	94.4%	100.0%	100.0%	97.8%	100.0%	100.0%	94.5%
2-Nitrophenol	−373.4%	−552.7%	80.3%	58.7%	60.8%	100.0%	77.6%	82.4%	99.4%
4-ethylphenol	64.4%	73.4%	99.0%	83.1%	88.8%	99.4%	82.8%	89.7%	99.8%
Naphthalene	19.0%	21.5%	55.6%	20.7%	42.4%	98.6%	35.2%	37.4%	98.2%
2-Nitrotoluene	−16.1%	13.3%	46.1%	56.5%	82.8%	96.2%	60.9%	72.4%	93.3%
O-VOCs	33.07%	55.04%	69.32%	89.93%	95.85%	98.35%	96.34%	92.03%	99.55%
VNCs	−84.64%	−96.75%	63.23%	66.96%	79.82%	98.10%	70.35%	69.29%	96.32%
VSCs	61.00%	56.96%	94.07%	35.51%	46.50%	93.06%	100.00%	100.00%	94.56%
t-VOCs	31.54%	47.80%	71.98%	86.10%	93.80%	97.56%	92.02%	88.83%	98.37%

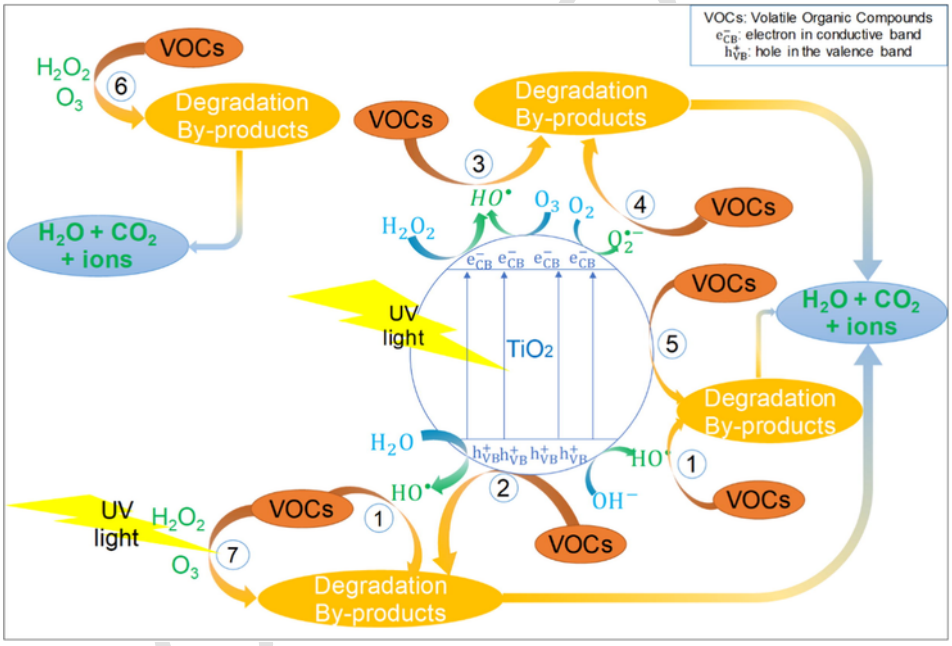

Fig. 2. Mechanism of the photocatalytic process aided with O_3, H_2O_2 and O_3/H_2O_2.

Toluene, 2-ethyl-1-hexanol, and phenol were purchased from POCH Poland; 1-nitropropane, heptylamine, 2-ethylthiophene, dibutyl sulfide, di-tert-butyldisulfide, pyridine and naphthalene from Sigma Aldrich and 4-ethylphenol was purchased from Acros organics (a POCH product). Benzene, o-xylene, ethylbenzene, nitrobenzene, 2-nitrophenol, 2-nitrotoluene, heptanoic acid, nonanoic acid, decanoic acid, 10-undecylenic acid, dodecanoic acid, furfural, m-cresol, o-cresol, acetophenone, tetrahydrofuran and 2-butanol were purchased from Merck (Germany).

2.2. Apparatus

To conduct the experiments, a pilot scale acid resistant steel closed cylindrical reactor was used, with a total volume of 15 dm^3 (Fig. 1S, Supporting Information (SI)). The details about the reactor are fully described in our previous work [48]. Additionally, to conduct the photocatalytic experiments, a UVHQ 250Z, Hg lamp from UV-technik (Germany), was connected to the reactor by one of lower windows of the reactor (Fig. 1S, number 2 and 3). The power of the lamp is 250 W, with a specific lamp power of 56 W/cm. A circulation of the model WW in the reactor through UV chamber was obtained by means of fluid-o-tech model MS 632–4 B34 pump (Italy) (Fig. 1S, number 4). The procedures were done in semi-batch mode where the oxidant was added in a continuous mode during the whole time of treatment. The model WW was pumped into the reactor by membrane (PTFE) pump model UGD 100/120-03, Euralca (Italy). H_2O_2, was fed to the reactor using a Hitachi LaChrom HPLC Pump model L-7110. Ozone was fed by a Tytan 32 Ozone generator that is able to produce up to 70 mg O_3/L of Oxygen. Dried air was used to produce Ozone. The separation be-

Table 3
Dissociation constant (pK_a) of the compounds composing the model WW.

Compound	pKa	reference
acetophenone	19	[63]
nonanoic acid	4.96	[64]
heptanoic acid	4.89	[64]
2-butanol	17.6	[64]
phenol	9.98	[64]
4-ethylphenol	10	[64]
heptylamine	10.67	[65]
pyridine	5.23	[66]
nitrobenzene	4.60	[67]
o-cresol	10.29	[64]
m-cresol	10.09	[64]
benzene	43	[68]
naphthalene	42	[68]
2-nitrophenol	7.23	[69]
1-nitropropane	9	[70]
decanoic acid	4.9	[64]
10-undecylenic acid	5	[64]
lauric acid	5.3	[64]
2-nitrotoluene	4.43	[67]
toluene	41	[71]
ehtylbenzene	36	[72]

tween the catalyst and the model WW taken in the samples collected was made by a Heraeus Sepatech centrifuge.

The detailed description of the apparatus for VOCs analysis by gas chromatography is described in our previous papers [49–51]. COD determination was done using a HACH COD reactor and a HACH DR/2010 spectrophotometer.

2.3. Procedure

2.3.1. Model wastewater

In order to simulate caustic effluents containing several VOCs present in a wide variety of industries, a model WW was prepared with the VOCs listed in Section 2.1 with a concentration around 40 ± 2 mg/L. The model WW has an initial pH of 11 and a measured COD between 2100 and 2300 mgO_2/L.

2.3.2. Wastewater treatment

To conduct all experiments performed, the model WW was prepared as followed; Firstly 5 dm^3 of deionized water at a pH of 10.5 (the pH of the deionized water was corrected with 0.1 M NaOH) was pumped to the reactor and heated until the desired temperature. Afterwards a known volume of primary solution was added by the special injection port, present in the reactor using a 10 ml gas tight syringe. The final concentration of each compound in the model WW was 40 ± 2 ppm. The initial pH was 11 in all procedures and no pH adjustment was performed during the treatment time. The stirring was established at 200 rotations per minute (rpm). After the model WW was prepared and at the desired operational conditions obtained, the catalyst was added by the upper part of the reactor and the recirculation pump was turned on. The catalyst was in contact with the model wastewater for 30 min before the beginning of the treatment. Samples were taken prior to catalyst addition and after the 30 min of contact to fully understand the influence of the adsorption phenomena on the concentration changes in primary WW. Regarding the oxidants used, the H_2O_2, the dose was establish depending on the mass ratio between the oxygen source provided by the oxidant and the COD of the model WW (r_{ox}) chosen. The detailed method to determine this ratio is provided in previous work [11]. This approach enables to optimize the amount of oxidant used. Table 1 presents the main parameters for the experiments (exp.) studied. The treatment time was set depending on the r_{ox}. The pH of collected samples was measured by non-bleeding pH strips (Merck).

2.3.3. Process control

Samples with a volume of 0.022 dm^3 were collected prior to catalyst addition and after the 30 min of contact with the catalyst. After the treatment started, samples were collected every 15 min in the first hour of treatment, at 90 min, 120 min and every hour until the end of the treatment. Samples were afterwards centrifuged for 20 min at 5000 rpm to obtain a good separation between treated effluent and catalyst. Every sample was taken with the purpose of analyzing the volatile organic compounds concentration, COD, and pH. COD was measured using the Polish standard test method PN-ISO 15705:2005, based on the dichromate method by HACH. Regarding the VOCs monitoring, the sample preparation was done by dispersive liquid-liquid micro-extraction (DLLME), the analysis of obtained extracts by means of Gas Chromatography-Mass spectrometry (GC–MS). Details of the procedures are fully described in our previous papers [49–51].

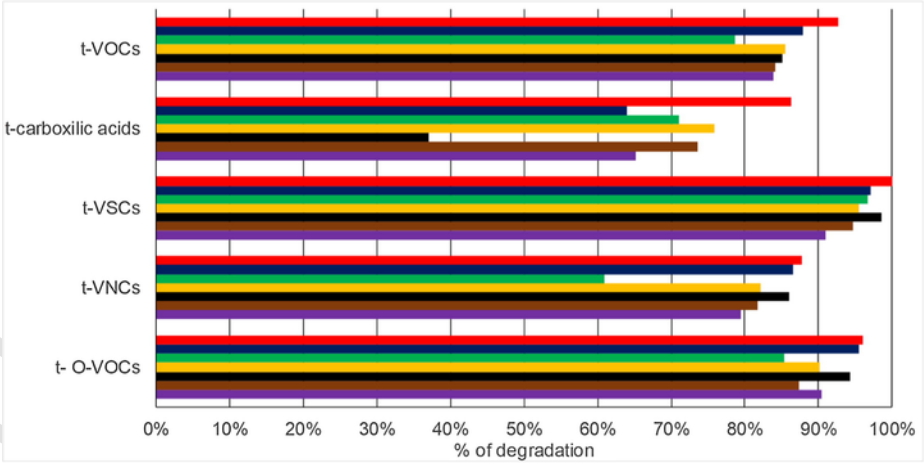

Fig. 3. Total-VSCs, VNCs, O-VOCs, carboxylic and total VOCs degradation in the TiO_2/UV/O_3 technologies. Purple columns, r_{ox} of 0.7 and a [TiO_2] of 100 mg/L; brown columns, r_{ox} of 0.70 and a [TiO_2] of 500 mg/L; black columns, r_{ox} of 0.70 and a [TiO_2] of 1000 mg/L; yellow columns, r_{ox} of 0.70 and a [TiO_2] of 2000 mg/L; blue columns, r_{ox} of 1.5 and a [TiO_2] of 500 mg/L; green columns, r_{ox} of 0.40 and a [TiO_2] of 500 mg/L; red columns, r_{ox} of 3.4 and a [TiO_2] of 500 mg/L. (For interpretation of the references to colour in this figure legend, the reader is referred to the web version of this article.)

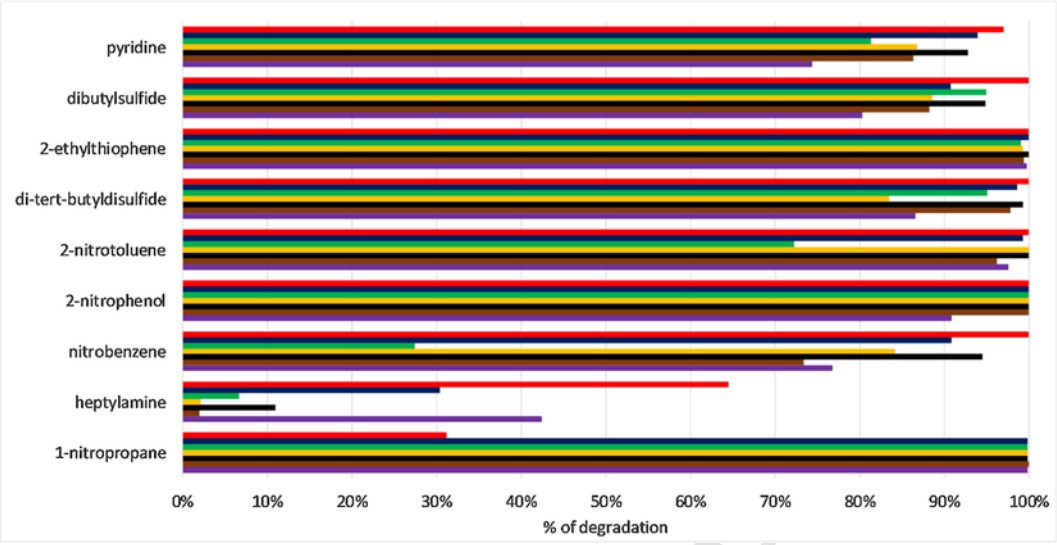

Fig. 4. Volatile nitrogen compounds and volatile sulfur compounds degradation using $TiO_2/UV/O_3$ processes. Purple columns, r_{ox} of 0.7 and a $[TiO_2]$ of 100 mg/L; brown columns, r_{ox} of 0.7 and a $[TiO_2]$ of 500 mg/L; black columns, r_{ox} of 0.7 and a $[TiO_2]$ of 1000 mg/L; yellow columns, r_{ox} of 0.7 and a $[TiO_2]$ of 2000 mg/L; blue columns, r_{ox} of 1.5 and a $[TiO_2]$ of 500 mg/L; green columns, r_{ox} of 0.4 and a $[TiO_2]$ of 500 mg/L; red columns, r_{ox} of 3.4 and a $[TiO_2]$ of 500 mg/L. (For interpretation of the references to colour in this figure legend, the reader is referred to the web version of this article.)

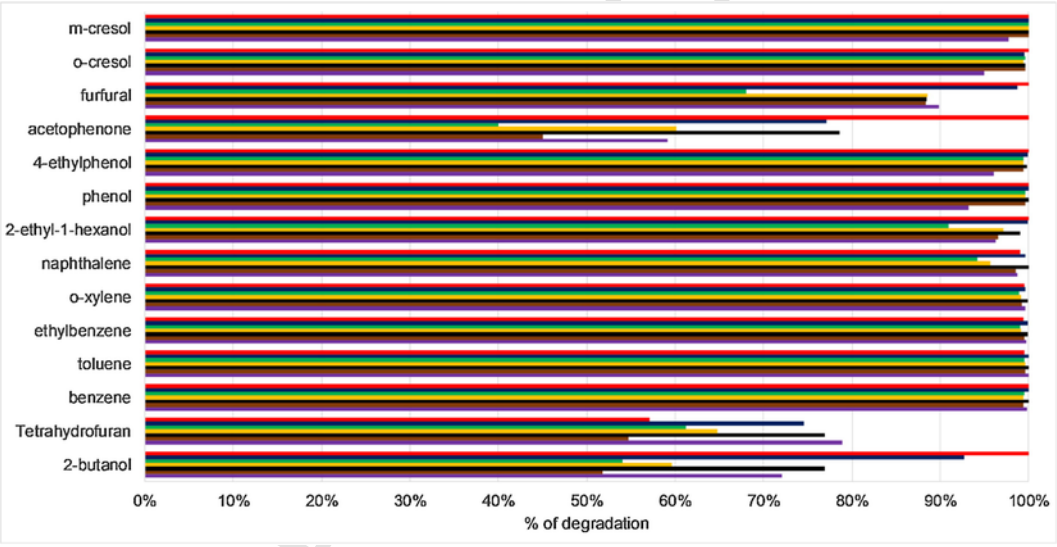

Fig. 5. Oxygen-volatile organic compounds degradation using $TiO_2/UV/O_3$ processes. Purple columns, r_{ox} of 0.7 and a $[TiO_2]$ of 100 mg/L; brown columns, r_{ox} of 0.7 and a $[TiO_2]$ of 500 mg/L; black columns, r_{ox} of 0.7 and a $[TiO_2]$ of 1000 mg/L; yellow columns, r_{ox} of 0.7 and a $[TiO_2]$ of 2000 mg/L; blue columns, r_{ox} of 1.5 and a $[TiO_2]$ of 500 mg/L; green columns, r_{ox} of 0.4 and a $[TiO_2]$ of 500 mg/L; red columns, r_{ox} of 3.4 and a $[TiO_2]$ of 500 mg/L. (double column). (For interpretation of the references to colour in this figure legend, the reader is referred to the web version of this article.)

3. Results and discussion

Experimental procedures were carried out using photocatalytic procedures assisted with external oxidants, namely, O_3, H_2O_2 and O_3/H_2O_2. To determine the effectiveness of the studied processes, control and monitoring during and after treatment of the VOCs present in the model WW was performed. In addition, the COD was analyzed before and after treatment for evaluation of changes of total pollution load (including possible by-products formed during oxidation). The dose of catalyst, the r_{ox} and adsorption are parameters under study.

Several types of VOCs were added into the caustic water matrix, including oxygenated volatile organic compounds (O-VOCs), volatile nitrogen compounds (VNCs), volatile sulfur compounds (VSCs) and carboxylic acids. The carboxylic acids are important compounds to study due to be part of the degradation pathway of some VOCs present in this work. There are evidences of the presence of carboxylic acids in the mineralization pathway of compounds like phenolic [13,52], nitrobenzene [53], toluene [54] and polyaromatic [55]. An alkaline water matrix was used to simulate caustic industrial WW and to check the performance of the photocatalytic processes under alkaline pH. In addition, there is an increase of the number of VOCs present and studied in the alkaline model WW, from 16 to 28 VOCs [48]. Nevertheless, the study can also be of an interest for other types of industrial effluents depending on the efficiency of the degradation of certain VOCs.

The selection of model compounds for this research was based on previous studies on treatment of real refinery effluents in basic pH conditions [11,12]. The compounds belong to different groups, covering a wide range of physiochemical properties and "reactivity" in terms of AOPs. The goal of this work was not to show 100% degradation of all

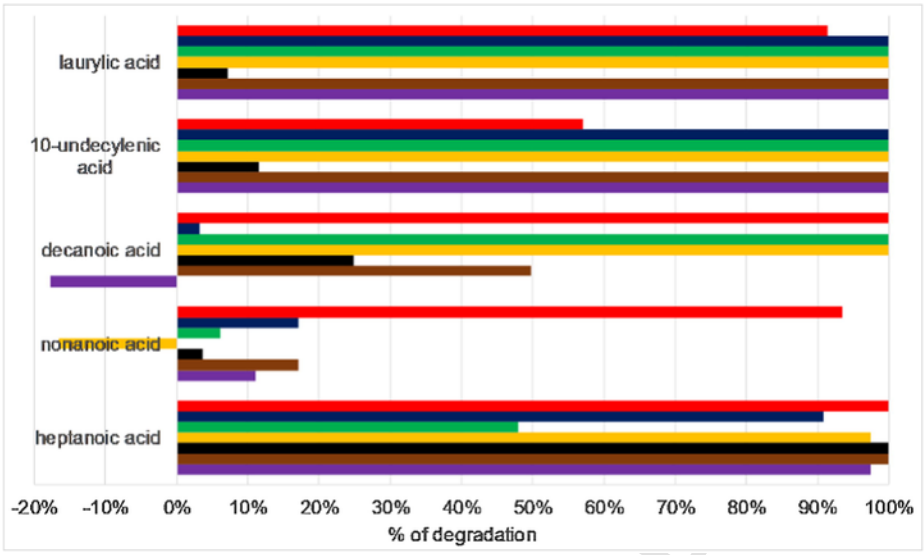

Fig. 6. Carboxylic acids degradation using $TiO_2/UV/O_3$ processes. Purple columns, r_{ox} of 0.7 and a $[TiO_2]$ of 100 mg/L; brown columns, r_{ox} of 0.7 and a $[TiO_2]$ of 500 mg/L; black columns, r_{ox} of 0.7 and a $[TiO_2]$ of 1000 mg/L; yellow columns, r_{ox} of 0.7 and a $[TiO_2]$ of 2000 mg/L; blue columns, r_{ox} of 1.5 and a $[TiO_2]$ of 500 mg/L; green columns, r_{ox} of 0.4 and a $[TiO_2]$ of 500 mg/L; red columns, r_{ox} of 3.4 and a $[TiO_2]$ of 500 mg/L.

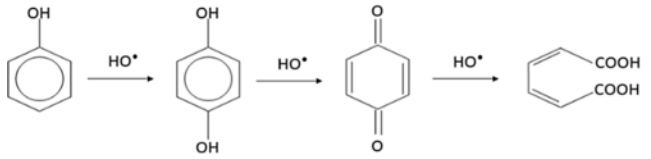

Diagram 1. Proposed mechanism for the degradation of phenol by ring cleavage resulting in formation of carboxylic acids [74].

model compounds allowing to state the complete success of the research. It was tried to perform a systematic evaluation of the performance of AOPs based on TiO_2. Thus, some model compounds are persistent to degradation and overall results of each group of studied processes strongly differs. This allows to perform a real evaluation of studied AOPs performance and highlight the challenges for further studies.

3.1. Performance evaluation of TiO_2

To understand the importance of the catalytic activity in the efficiency of the studied processes, non-irradiated and UV irradiated O_3, H_2O_2 and O_3/H_2O_2 processes were also performed keeping the same operational parameters as of the photocatalytic processes. Fig. 1 and Table 2 depict the degradation of the O-VOCs, VNCs, VSCs and total VOCs (t-VOCs) in each process. Compounds like, 2-nitrophenol, naphthalene, 2-nitrotoluene, dibutyl-sulfide and ethylbenzene exhibit significant improvement in their degradation when TiO_2 was added in the process as illustrated in Figs. 2S and 3S. Looking to Fig. 5S, these compounds reveal to have significant adsorption to the TiO_2 surface, contributing for the degradation increase of the listed compounds. These studies revealed, that the TiO_2 can increase the degradation of the VOCs in general, when comparing with UV related and non-catalytic processes. This can be related with the higher yield of $HO^{\bullet}$ produced at the catalyst surface as illustrated in Fig. 2 (reactions (1)–(4)). As stated in introduction section, the irradiation of TiO_2, enables an electron (e^-) to be conducted from its VB to the CB with the consequent formation

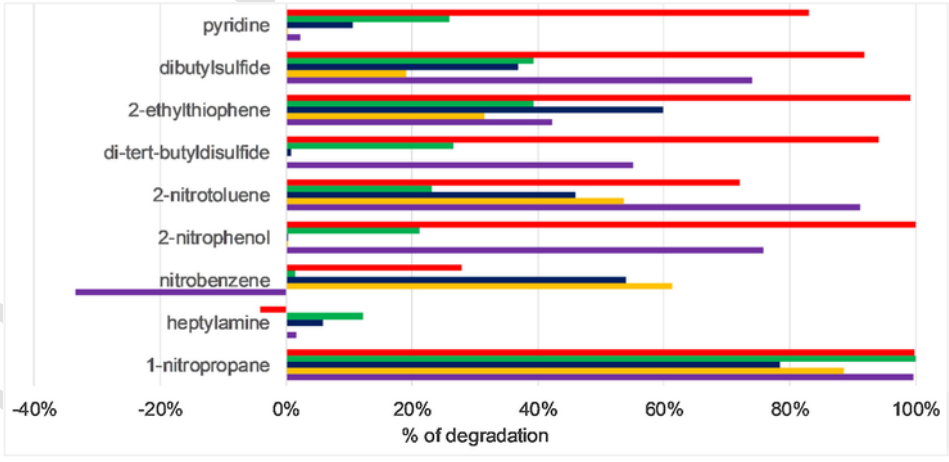

Fig. 7. Volatile nitrogen compounds and volatile sulfur compounds degradation using $TiO_2/UV/H_2O_2$ processes. Purple columns, r_{ox} of 0.5 and a $[TiO_2]$ of 100 mg/L; yellow columns, r_{ox} of 0.5 and a $[TiO_2]$ of 500 mg/L; blue columns, r_{ox} of 0.5 and a $[TiO_2]$ of 1000 mg/L; green columns, r_{ox} of 0.27 and a $[TiO_2]$ of 100 mg/L; red columns, r_{ox} of 1.111 and a $[TiO_2]$ of 100 mg/L. (For interpretation of the references to colour in this figure legend, the reader is referred to the web version of this article.)

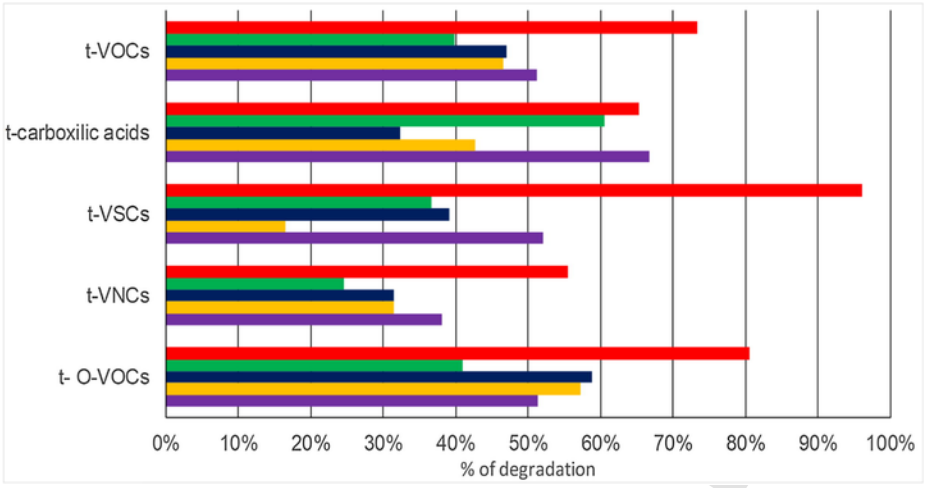

Fig. 8. Total-VSCs, VNCs, O-VOCs, carboxylic and total VOCs degradation in the $TiO_2/UV/H_2O_2$ technologies. Purple columns, r_{ox} of 0.5 and a $[TiO_2]$ of 100 mg/L; yellow columns, r_{ox} of 0.5 and a $[TiO_2]$ of 500 mg/L; blue columns, r_{ox} of 0.5 and a $[TiO_2]$ of 1000 mg/L; green columns, r_{ox} of 0.27 and a $[TiO_2]$ of 100 mg/L; red columns, r_{ox} of 1.1 and a $[TiO_2]$ of 100 mg/L.

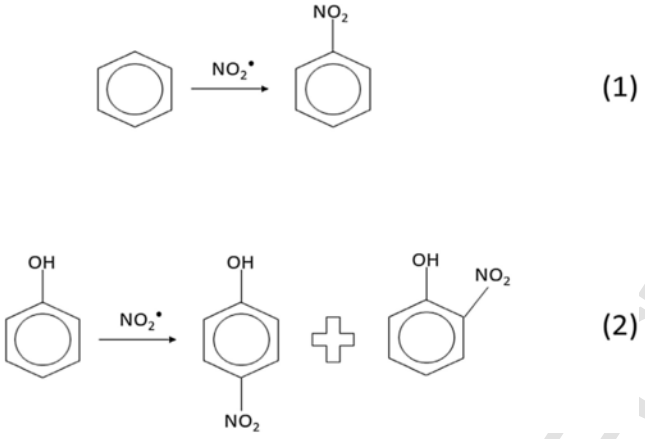

Diagram 2. Proposed mechanism for the nitration of benzene and phenol rings to synthetize nitrobenzene (1) [48,81] and 2-nitrophenol/4-nitrophenol (2) [82].

of holes in the VB (h_{VB}^+) that will act as oxidizing sites as described in Eq. (1) [56–58].

$$SMP \xrightarrow{h\upsilon} SMP\left(e_{CB}^- + h_{VB}^+\right) \quad (1)$$

In presence of h_{VB}^+, the surface adsorbed H_2O and OH^- can act as electron donors leading to the formation of $HO^{\bullet}$, demonstrated in Eqs. (2) and (3) [22] and in Fig. 2 (reaction (1)).

$$h_{VB}^+ + H_2O \rightarrow HO^{\bullet} + H^+ \quad (2)$$

$$h_{VB}^+ + OH^- \rightarrow HO^{\bullet} \quad (3)$$

In addition, it is possible that the VOCs can be oxidized by the h_{VB}^+ [59,60] as described in reaction (2) in Fig. 2. When ozone (O_3) or hydrogen peroxide (H_2O_2) are in the bulk solution they will act as e^- acceptors reacting with the electron in the conduction band and generating $HO^{\bullet}$, as described in Eqs. (4) and (5) [61,62] and illustrated in Fig. 2 (reaction (3)).

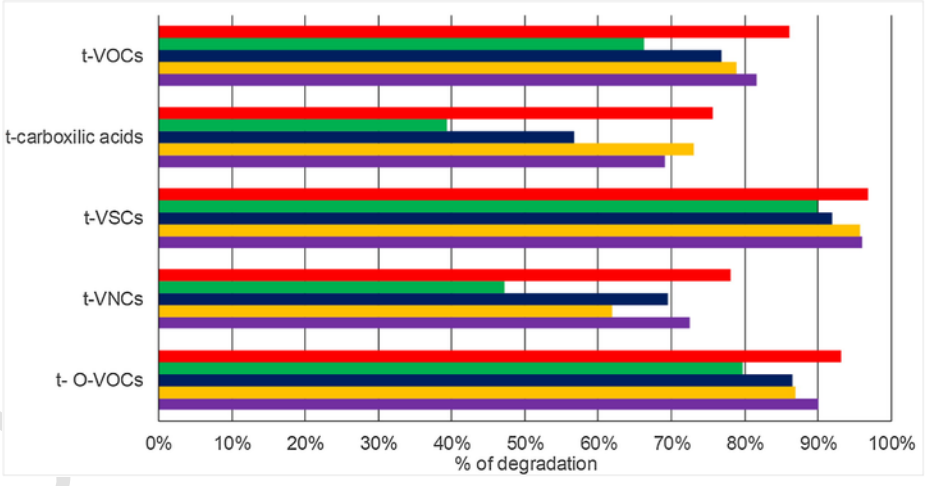

Fig. 9. Total-VSCs, VNCs, O-VOCs, carboxylic and total VOCs degradation in the $TiO_2/UV/O_3/H_2O_2$ technologies. Purple columns, r_{ox} of 0.5 and a $[TiO_2]$ of 100 mg/L; yellow columns, r_{ox} of 0.50 and a $[TiO_2]$ of 500 mg/L; blue columns, r_{ox} of 0.50 and a $[TiO_2]$ of 1000 mg/L; green columns, r_{ox} of 0.26 and a $[TiO_2]$ of 100 mg/L; red columns, r_{ox} of 1.1 and a $[TiO_2]$ of 100 mg/L

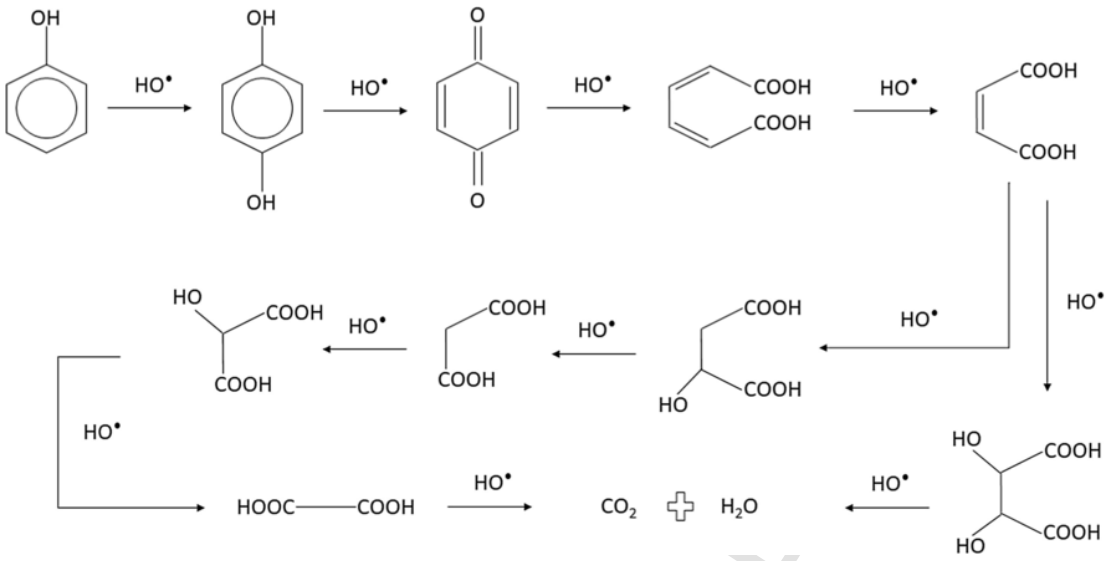

Diagram 3. Proposed mechanism for the degradation of phenol to full mineralization. Degradation though carboxylation via $HO^{\bullet}$ reducing the carbon chain of the carboxylic acids to simpler acids and to CO_2 and H_2O [86–89].

Table 4
Calculations to determine the cost of process of all technologies studied.

N° of exp.	Process	t (min)	Oxidant Amount (g)	TiO_2 amount (g)	Equipment cost ($)	Maintenance cost/year($)	chemical cost ($/m^3)	energy demand (kJ)	energy cost/ batch ($/)	energy cost ($/m^3)	Operation cost ($/m^3)
1	$TiO_2/UV/O_3$	100	12	0.5	12,789	384	0.003	4200	0.128	25.67	25.67
2	$TiO_2/UV/O_3$	100	12	2.5	12,789	384	0.015	4200	0.128	25.67	25.68
3	$TiO_2/UV/O_3$	100	12	5	12,789	384	0.030	4200	0.128	25.67	25.70
4	$TiO_2/UV/O_3$	100	12	10	12,789	384	0.060	4200	0.128	25.67	25.73
5	$TiO_2/UV/O_3$	60	9.54	2.5	12,789	384	0.015	2520	0.077	15.40	15.42
6	$TiO_2/UV/O_3$	95	6	2.5	12,789	384	0.015	3990	0.122	24.38	24.40
7	$TiO_2/UV/O_3$	120	19.08	2.5	12,789	384	0.015	5040	0.154	30.80	30.82
22	O_3	100	12	–	12,600	378	–	2700	0.083	16.50	16.50
23	O_3/UV	15	1.8	–	12,789	384	–	630	0.019	3.85	3.85
13	$TiO_2/UV/O_3/H_2O_2$	95	O_3: 5.92 H_2O_2: 1.78	0.5	14,789	444	0.181	4446	0.136	27.17	27.35
14	$TiO_2/UV/O_3/H_2O_2$	95	O_3: 5.92 H_2O_2: 1.78	2.5	14,789	444	0.193	4446	0.136	27.17	27.36
17	$TiO_2/UV/O_3/H_2O_2$	60	O_3: 7.2 H_2O_2: 2.16	0.5	14,789	444	0.219	2808	0.086	17.16	17.38
24	O_3/H_2O_2	60	O_3: 5.92 H_2O_2: 1.78	–	14,600	438	0.178	1908	0.058	11.66	11.84
25	$O_3/H_2O_2/UV$	60	O_3: 5.92 H_2O_2: 1.78	–	14,789	444	0.178	2808	0.086	17.16	17.34

$$O_3 + e_{CB}^- + H_2O \rightarrow OH^- + HO^{\bullet} + O_2 \quad (4)$$

$$H_2O_2 + e_{CB}^- \rightarrow HO^{\bullet} + OH^- \quad (5)$$

Furthermore, oxygen (O_2) can also generate other reactive species like superoxide radical anion upon reaction with e^- (Eq. (6)) (Fig. 2, reaction (4)).

$$O_2 + e_{CB}^- \rightarrow O_2^- \quad (6)$$

A comprehensive analysis of the effectiveness and differences in the treatment of the model WW is accompanied by the results of COD reduction of the studied processes (Table 1 and Fig. 4S). It can be seen that photocatalytic AOPs can increase the treatment efficiency, with a higher COD reduction. Non-catalytic processes obtain less COD reduction than photocatalytic processes. Also in the case of H_2O_2 and O_3 assisted photocatalytic processes, higher COD reduction was achieved when comparing with H_2O_2/UV and O_3/UV. This proves the catalyst influence on the treatment efficiency even in basic pH conditions. In the case of O_3/H_2O_2 assisted photocatalytic processes, $O_3/H_2O_2/UV$ achieved slightly higher COD reduction, in contrast with the other cases. Other explanation relates to the fact that radicals formed at the catalyst surface can react with O_3 and H_2O_2 instead of the VOCs, generating less reactive species and consequently generating a negative impact on the COD reduction of the model WW. To conclude, it was proven that TiO_2 and photocatalytic AOPs influences positively the treatment of the selected VOCs comparing with non-catalytic AOPs and have been further studied and explained in the next sections.

3.2. Adsorption studies

To obtain a better insight regarding the interaction between the catalyst and the VOCs present in the model WW, adsorption studies were performed. The catalyst was left in contact with the model WW without any irradiation and oxidant addition for 150 min. Two different concentrations of TiO_2 (100 and 500 mg/L) were used. The initial pH

was 11 and kept constant during the contact time, which means that the TiO_2 surface was negatively charged (PZC = 6.25) [34]. The identification and quantification of the VOCs after the contact time is presented in Fig. 5S. Table 3 illustrates the pKa of the compounds present in the model WW that can explain their behavior in the adsorption studies. The results clearly illustrate that the compounds that had significant percentage of adsorption also had high degradation efficiencies such as 1-nitropropane, dibutylsulfide, decanoic acid and BTEX. These studies revealed that the adsorption on the catalyst surface is a limiting stage for effective oxidation by the studied photocatalytic processes. This is the main place of their oxidation. Reaction in the bulk solution in the case of compounds having good adsorption on TiO_2 has secondary importance on the final effectiveness. This happens due to the interaction between the negatively charged surface of the TiO_2 and the compounds present in the medium. Majority of them are in their neutral or anionic form, thus limiting the adsorption on the catalyst surface.

In contrast, the compounds which were more persistent to degradation, e.g., heptylamine (pKa = 10.7), acetophenone (pKa = 19), nonanoic acid (pKa = 4.96), 2-butanol (pKa 17.6) and tetrahydrofuran had low adsorption (bellow 6%) to the surface of TiO_2. Regarding heptylamine, nonanoic acid and tetrahydrofuran at the pH used (11) in this work, they are in their anionic form (nonanoic acid) or neutral form (heptylamine) which will generate repulsing interactions (in respect to heptylamine by electron pairs of the amine group) with the negatively charged surface of TiO_2, thus inhibiting their adsorption. In contrast, acetophenone and 2-butanol at pH 11 are in their neutral state, thus in some manner they are also not strongly attracted to interact with the negatively charged surface of TiO_2. These reasons sustain a lower interaction with the surface of the catalyst and therefore is more likely to have lower percentage of degradation than the other VOCs. The reactions with oxidants and their radical forms will take place mainly in the bulk of the solution as illustrated in Fig. 2 (reactions 6 and 7).

An interesting behavior is that O-VOCs and VSCs had higher adsorption with a TiO_2 of 100 mg/L than 500 mg/L, while carboxylic acids had a significant increase on their adsorption percentage at 500 mg/L of TiO_2. This behavior goes on the opposite direction than the theoretical hypothesis. A possible explanation or hypothesis is related to the phenomenon of multilayer adsorption formed in the case of lower TiO_2 concentration. This multilayer formed by carboxylic acids interacts with other compounds in the bulk, thus increasing their sorption. At higher concentration of TiO_2, the concentration of carboxylic acids in the bulk is lowered, thus the multilayer is not formed, thus finally lower amount of other groups of compounds exhibits sorptive interactions. These studies suggest that the degradation of VOCs on the TiO_2 surface has a poor impact on the overall degradation of the VOCs, resulting in a high dependence of the VOCs degradation taking place in the bulk solution. The role of the catalyst in this case is to effectively activate the oxidant by photochemical reactions on its surface to produce hydroxyl radicals which further go on reaction with the pollutants in the bulk solution.

3.3. Photocatalytic processes using TiO_2 assisted with O_3

The treatment of the model WW was carried out using photocatalytic processes based on TiO_2 (TiO_2/UV) and assisted by O_3 (TiO_2/UV/O_3) at different TiO_2 concentrations. The effect of the TiO_2 concentration was studied using 4 different levels, i.e., 100, 500, 1000 and 2000 mg/L (Fig. 3 and Table 1). The obtained results reveal that the increase of the catalyst concentration, in the case of sole UV/TiO_2 processes, had no significant effect on the VOCs degradation and COD reduction. Some specific groups of VOCs can have a direct relation between adsorption phenomena and the degradation efficiency. For example, carboxylic acids degradation is higher at 500 mg/L of TiO_2 (74%; exp. 2 Table 1) than at 100 mg/L of TiO_2 (65%; exp. 1 Table 1), which can be related to the higher adsorption of the majority of carboxylic acids (decanoic, laurylic and 10-undecylenic acid) (Fig. 5S). This behavior can be related with the following hypothesis. First, the TiO_2 is in fact being activated by the UV light but the TiO_2 surface charge at the basic pH conditions is equal to the charge of the majority of the VOCs. This is influenced by the pKa of the VOCs, the PCZ of theTiO_2 and the pH of the medium. Secondly, and in connection with the first hypothesis, the pH of the medium negatively affects the adsorption of the VOCs to the catalyst surface. The PZC of the TiO_2 is 6.25 [42] which means that at the beginning of the treatment with a pH of around 11, the surface of the catalyst is negatively charged. With the treatment time the pH decreased to neutral values allowing the surface charge of the catalyst to change to neutral or even positive charge which can enhance the possibilities of adsorption of the VOCs.

Regarding the VOCs degradation in details, Fig. 4 shows the degradation of VSCs and VNCs using TiO_2/O_3/UV. VSCs were effectively degraded with exception of dibutylsulfide in exp. 2 from Table 1 with 56% of degradation. No major difference was observed in the degradation of the VSCs when doubling the r_{ox} or the catalyst dose. Nevertheless, TiO_2/O_3/UV, using a r_{ox} = 0.39 and TiO_2 = 500 mg/L (exp. 6 Table 1), was the most efficient process with 97% degradation of the total VSCs (Fig. 3).

In terms of VNCs, heptylamine was persistent to degradation in all processes studied. Its chemical composition can explain such a behavior – it is not an aromatic compound and does not contain any double bonds.

In addition, it was proved that the reaction rate constant with ozone decreases from tertiary to simple amines and were lower than phenol and therefore most likely decreased the degradation of the contaminants studied [73]. An increase of the r_{ox} from 0.69 to 3.44 (exp. 2, 5 and 7 from Table 1) has minor effect of the effectiveness of some VNCs like nitrobenzene and 2-nitrotoluene. No major difference between the rest of the process studied, with a difference of 6% between a r_{ox} of 3.44 and 0.69. The TiO_2/UV/O_3 (Table 1, exp. 2) (0.70 r_{ox}; 500 mgTiO_2/L) was the most efficient.

Fig. 5 describes in detail the O-VOCs degradation, and it allows to identify some compounds that did not reach total degradation. Acetophenone, tetrahydrofuran and 2-butanol were the compounds identified as persistent to degradation, effectively degraded only with a higher r_{ox} applied (exp. 7, Table 1). High pKa of acetophenone (19) can explain the low degradation. Similar results were obtained in a previous study of acetophenone degradation by TiO_2 based photocatalytic process [74]. Non-aromatic compounds such as 2-butanol and tetrahydrofuran were the most resistant to be degraded. The remaining compounds, like BTEX, phenolic and polyaromatic compounds achieved almost complete degradation in all processes. The TiO_2/UV/O_3 (experiment no. 3) (r_{ox} of 0.7 and 1000 mgTiO_2/L) was the most efficient process to degrade O-VOCs.

Fig. 6 shows in detail the degradation of carboxylic acids. Nonanoic and decanoic acids were persistent to degradation and in some cases their concentration increased. This can be related with the degradation of the other VOCs. It is known that carboxylic acids are formed as a result of the oxidation via $HO^{\bullet}$ of compounds like, phenol [75], nitrobenzene[53], naphthalene based compounds like dyes [55] and BTEX [76]. Carboxylic acids are usually generated when the aromatic ring is cleaved via $HO^{\bullet}$ [74]. This mechanism is illustrated in Diagram 1. Other carboxylic acids were effectively degraded. The results proved that in fact there is a linkage between the aromatic compounds and the carboxylic acids, and also that this type of AOPs is effective in degrading several types of carboxylic acids, enabling further degradation of the VOCs attempting full mineralization. The experiment 7 (Table 1: r_{ox} of 3.44; 500 mg TiO_2/L) was the most effective to degrade all the acids

studied with 86% of degradation but experiment 2 (Table 1: r_{ox} of 0.69; 500 mg TiO_2/L) allowed to obtain only slightly lower total effectiveness −74% resulting in the optimal process to degrade carboxylic acids. This result was affected mainly due to the low degradation of the nonanoic acid.

Regarding the t-VOCs degradation, Fig. 3 shows that the highest efficiency was obtained in $TiO_2/UV/O_3$ (exp. 7) with 93% of t-VOCs. Keeping the r_{ox} constant, TiO2/UV/O3 (exp. 4) was considered the most efficient process obtaining 86% degradation of t-VOCs. With a significant lower dose of TiO_2 (500 mg/L) and r_{ox} (0.68), 84% degradation of t-VOCs was still obtained. Taking into account that the goal is to use the less amount of oxidant and catalyst possible and to obtain highest efficiency possible, the optimal process was achieved in $TiO_2/UV/O_3$ (exp. 2) (Table 1: r_{ox} of 0.70; 500 mg TiO_2/L).

Table 1 also reveals the effect of the r_{ox} value. It is clear that this effect generates changes in the COD reduction. While keeping the TiO_2 constant at 500 mg/L, reducing the r_{ox} from to 0.70 to 0.40, a 4% reduction in COD was noted – from 44 to 40% in TiO2/UV/O3 (exp. 2 and 6, Table 1). In $TiO_2/UV/O_3$(exp. 6), the efficiency of oxidation reaches nearly 100% – this situation is optimal in terms of oxidant utilization. In contrast, when increasing the r_{ox} from 0.69 to 1.51 and 3.44, the COD reduction increased from 44 to 55 and 66%, respectively (exp. 5–7, Table 1).

There is a need to double the value of r_{ox} (the double of the oxidant dose) to obtain approx. 10% increase in the COD reduction. It is clear that a percentage of the compounds that represent the remaining COD of the model WW is not effectively degradable via AOPs. Fig. 6S depicts that COD reduction happens mainly is the first 30 min of treatment and in this time the pH drastically reduces to values around 7, which is close to the PZC. After this time the pH goes below the PZC, which results in change of the surface charge of the TiO_2 from negative to neutral or positive value. In addition, the influence of the alkaline pH in the oxidation of O_3 stops and the oxidation occurs mainly assisted with UV and photocatalytic activity. Furthermore, at 30 min of treatment, the majority of the VOCs studied were effectively degraded (above 80%), with exception of acetophenone, 2-butanol, heptylamine, nitrobenzene and some carboxylic acids that did not reach high degradation at 30 min of treatment time. These facts can sustain why the COD reduction is significantly lower than in the first 30 min. The COD reduction rate decreases after the majority of the VOCs were degraded under the LOD.

3.4. Photocatalytic process using TiO_2 assisted with H_2O_2

H_2O_2 is one of the most widely used oxidants and has been considered to be safe due to the formation of water as its final product. Therefore, its role on the photocatalytic degradation of VOCs was thoroughly assessed. The H_2O_2, when present in the medium, is converted to $HO^{\bullet}$ either directly by the UV radiation or can react on the surface of the catalyst [42]. The effect of the catalyst concentration and r_{ox} on VOCs degradation, COD content and pH variation during treatment were evaluated.

The analysis of the VOCs monitoring revealed a significant differences comparing with $TiO_2/UV/O_3$ as demonstrated in Fig. 7. Analyzing the VSCs, it is clear that they were only effectively degraded in experiment 11 (Table 1 and Fig. 8: r_{ox} of 1.1; 100 mg TiO_2/L). The use of H_2O_2 was less effective comparing to O_3 in the photocatalytic process using TiO_2. Previously, similar results were obtained for non-catalytic [11,12] and cavitation based processes [77–79]. In terms of VNCs and likewise in the $TiO_2/UV/O_3$, heptylamine was persistent to degradation in all processes. In the case of $TiO_2/UV/H_2O_2$, nitrobenzene was also more persistent to degradation. In experiment 8 (Table 1 and Fig. 8: r_{ox} of 0.50; 100 mg TiO_2/L) the nitrobenzene concentration increased by 33% as illustrated in Fig. 8. A possible hypothesis for this increase can be related with the degradation pathway of benzene that could possibly generate nitrobenzene. In recent studies, it was revealed that 2-nitrophenol (mechanism 2, Diagram 2) and nitrobenzene (mechanism 1, Diagram 2) derivatives can be formed from nitrate and nitrite group formed which "attack" the aromatic ring of benzene or phenol [48,80,81] as demonstrated in Diagram 2. In this case, this happens due to nitrite ions formation from N_2 in the presence of H_2O_2. Even though this reaction occurs at a very low rate, only a small amount of nitrite is needed to trigger the reaction [82,83]. Even though the reactor is closed during the experiments, but the air is present inside which includes molecular nitrogen (N_2). Interestingly, 1-nitropropane was effectively degraded by all processes studied in contrast with other compounds that have more affinity with the "attack" of $HO^{\bullet}$. This compound was persistent to degradation and consider as a by-product of degradation of other and more complex VNCs in a previous work, using real industrial effluents [11]. What is important here to take into consideration is that this type of AOP is able to also degrade short chain and non-aromatic compounds, enabling to achieve complete mineralization. In $TiO_2/UV/H_2O_2$ (Exp. 11 (Table 1 and Fig. 8: r_{ox} of 1.1; 100 mgTiO_2/L) was the best choice to degrade VSCs and VNCs.

Regarding the O-VOCs and with similar behavior of $TiO_2/UV/O_3$, it is clear that compounds like tetrahydrofuran, 2-butanol, acetophenone and furfural were more persistent to degradation, with the first three compounds having their degradation below 50% in all processes (Fig. 7S). The remaining compounds, with exception of 2-ethyl-1-hexanol, are aromatic and were effectively degraded especially in experiment 11 (Table 1 and Fig. 7S: r_{ox} of 1.1; 100 mgTiO_2/L), consistent with the results of $TiO_2/UV/O_3$. Keeping the r_{ox} constant 0.50, the optimal [TiO_2] for O-VOCs was 500 mg/L, achieving 57% of O-VOCs degradation. Since the optimal [TiO_2] was chosen taking into account the t-VOCs, the concentration chosen was 100 mg/L and the optimal process was achieved in experiment 11 (Table 1 and Fig. 7: r_{ox} of 1.1; 100 mgTiO_2/L), achieving 81% of O-VOCs degradation.

In respect to the carboxylic acids, nonanoic acid was poorly degraded in all processes (Fig. 8S). Laurylic acid was effectively degraded in the processes using a [TiO_2] of 100 mg/L. When increasing the dose of TiO_2 the scenario changed with a negative degradation, meaning that Laurylic acid is a by-product of other compounds present in the model WW that were degraded with the increase of the [TiO_2]. Overall, the most efficient process was achieved in $TiO_2/UV/H_2O_2$, experiment 8 ((Table 1 and Fig. 4: r_{ox} of 0.50; 100 mgTiO_2/L) In these processes, the carboxylic acids are present in the pathways of degradation of the other and more complex VOCs, due to the mechanism based on the cleavage of the aromatic ring of the majority of the compounds studied in this work, as illustrated in Diagram 1.

The most efficient concentration of TiO_2 was 100 mg/L with 51% degradation of the t-VOCs and the optimal process to degrade the model WW was obtained in $TiO_2/UV/H_2O_2$ experiment 11 (Table 1 and Fig. 4: r_{ox} of 1.1; 100 mg TiO_2/L) with 73% degradation of t-VOCs.

Table 1 summarizes the COD reduction results from $TiO_2/UV/H_2O_2$ experiments studied. When the [TiO_2] was kept at 100 mg/L and the r_{ox} value was changed, a significant difference were observed. When the r_{ox} was decreased by approximately half (from 0.49 to 0.27), the COD reduction decreased from 13 to 8%, which makes the dose of oxidant crucial for the degradation of the model WW. Furthermore, when the r_{ox} increased from 0.49 to 1.12, the COD reduction only increased from 13 to 18%. This suggest a poor efficiency in degrading the organic load of the model WW. Not only the TiO_2 photocatalytic process is weak but also the oxidant used was not efficient in the operational conditions used in this work. The sole use of H_2O_2 was reported to be not efficient in the degradation of VOCs in a model caustic WW [48] and in real industrial effluents [11]. In addition, Fig. 9S presents the results of COD reduction and the changes in the pH during the treatment process. It clearly reveals that, likewise in the $TiO_2/UV/O_3$, there

is no effect of the TiO_2 concentration on the COD and the final pH changes. The same explanation described in the previous section for the $TiO_2/UV/O_3$ processes can be given here. It is related with the pH value of the model WW, which makes the surface of TiO_2 negative (PZC = 6.25) and pKa of the compounds, which will define if they are in their cationic, anionic or neutral state at the pH of the model WW. The experiment 11 (Table 1: r_{ox} of 1.1; 100 mgTiO_2/L) was the best $TiO_2/UV/H_2O_2$ process with 18% of COD reduction.

3.5. Photocatalytic process using TiO_2 assisted with O_3/H_2O_2

The combination of O_3 and H_2O_2 is often as an advanced oxidation technology which produces higher amount of $HO^{\bullet}$ as compared to either one of them alone [84]. The combination of both of these oxidants (i.e., O_3 and H_2O_2) with UV/TiO_2 could enhance the removal efficiency of target pollutants through formation of higher $HO^{\bullet}$ concentration.

No impact of TiO_2 concentration in the range of 100–1000 mg/L was observed using $TiO_2/UV/O_3/H_2O_2$ process for VOCs degradation (Fig. 9). Analyzing the VSCs, the increase of the r_{ox} from 0.50 to 1.10, while keeping the [TiO_2] constant at 100 mg/L, did not led to an increase of the degradation, showing that there is no further oxidation of the VSCs is possible via these processes. The optimal process to treat the VSCs demands relatively low amounts of catalyst and oxidants – suggesting the experiment 13 (Table 1, Figs. 9 and 10S: r_{ox} of 0.50; 100 mg TiO_2/L) has the optimal operational conditions.

The degradation of the VNCs is similar to the $TiO_2/UV/O_3$ process. Heptylamine was persistent to oxidation in all processes. It is clear that this compound is hard to degrade by all processes studied in this work or it is a by-product of the oxidation of other more complex compound. Nitrobenzene had a degradation around 50% in the most efficient processes and did not go for further degradation. One of the hypothesis can be related with the formation of nitrobenzene via the addition of the nitro group to the benzene ring [82]. This nitrogen group can be formed by irradiation of nitrite, which can be formed from oxidation of nitrogen molecule present in the aqueous media [83], the nitrogen is introduced along with ozone, which is generated from the dry air stream. In a previous work, same persistency of nitrobenzene to degradation using peroxone was reported [48].In a similar way to the other technologies studied in this work, 1-nitropropane was completely degraded. Overall, for VNCs, the most efficient TiO_2 concentration was 100 mg/L with 73% degradation using a r_{ox} of 0.50 (Figs. 9S and 10S). The optimal r_{ox} value was 0.50 due to the small increase of the degradation of the VNCs from 73 to 78% when increasing the r_{ox} to 1.1. Thus, $TiO_2/UV/O_3/H_2O_2$ experiment 13 (Table 1 and Fig. 9: r_{ox} of 0.50; 100 mg TiO_2/L) was the optimal process to degrade VNCs.

Regarding the O-VOCs, the results indicate a similar degradation profile to $TiO_2/UV/O_3$ process with acetophenone, tetrahydrofuran and 2-butanol revealing more persistency to oxidation (Fig. 11S). All these compounds, as described in Section 3.3, are non-aromatic in nature, with the exception of acetophenone, and can be one of the reasons for such decrease in their degradation. This is because, $HO^{\bullet}$ have a higher ability to react with double bounds and aromatic rings than with simple chain compounds [85]. The experiment 13 (Table 1 and Fi. 9: r_{ox} of 0.50; 100 mgTiO_2/L) was once more the optimal process, to degrade the O-VOCs with 90%.

$TiO_2/UV/O_3/H_2O_2$ process was found to be effective in carboxylic acids degradation (Fig. 12S). In similar trend with the other technologies studied, nonanoic and decanoic acid were more persistent to degradation. By changing r_{ox} from 0.50 to 1.10 with a [TiO_2] of 100 mg/L, carboxylic acids degradation decreased except nonanoic acid. This can be related with the higher degradation of the other compounds present (O-VOCs, VNCs and VSCs) which will generate decanoic or heptanoic acids. Further decrease in r_{ox} from 0.50 to 0.26 resulted in significant decrease of carboxylic acids degradation, probably due to the less amount of oxidants to generate sufficient $HO^{\bullet}$. Since all of the carboxylic acids are simple chain carbon compounds, with exception to 10-undecylenic acid, the $HO^{\bullet}$ prefers to "attack" double bonds and aromatic compounds due to their electron donor capabilities. The degradation of the carboxylic acids via $HO^{\bullet}$ takes place via hydroxylation and decarboxylation processes in the carbon chains, which will step-by-step produce CO_2 and H_2O reducing the carbon chain producing smaller chain acids, ketones or even aldehydes [86–89]. This mechanism is detailed illustrated in Diagram 3. The chain will be slowly reduced until its complete degradation generating CO_2 and H_2O. As clearly shown in Fig. 12S, only 10-undecylenic acid was fully degraded in all processes studied in this work, probably due to its double chain in the edge of the compound. Experiment 14 (Table 1 and Fig. 9: r_{ox} of 0.50; 500 mgTiO_2/L) was the most efficient process with 73% of degradation. Nevertheless, experiment 13 (Table 1 and Fig. 9: r_{ox} of 0.50; 100 mgTiO_2/L) allows to obtain a 69% of degradation of all carboxylic acids, thus this process should be considered as the most optimal configuration of the process parameters.

Carefully analyzing the Fig. 9, experiment 13 (Table 1: r_{ox} of 0.50; 100 mg TiO_2/L) was the optimal process to degrade the studied VOCs, with 82% of total-VOCs degradation.

COD reduction of the model WW using $TiO_2/UV/O_3/H_2O_2$ is summarized in Table 1. The effect of TiO_2 concentration (100 to 1000 mg/L) employing r_{ox} = 0.51 (exp. 13 to 15, Table 1), had minor influence on the COD reduction. Thus, the optimal concentration was 100 mg/L and was used in the studies of the effect of the r_{ox}. With a r_{ox} of 0.26, 26% of COD reduction was obtained indicating very good effectiveness of the added oxidant. Increasing the r_{ox} value from 0.26 to 0.49 and 1.12, the COD reduction increased to 38 and 43%, respectively. This proves that the increase of the r_{ox} is not giving a linear increase on the COD reduction. In addition, the majority of the oxidant added was not used to degrade the organic load of the model WW or that part of the COD in the form of by-product is persistent to degradation and cannot be effectively degraded via this technology. Therefore, the experiment 13 (Table 1: r_{ox} of 0.50; 100 mgTiO_2/L) was considered the optimal process to obtain an effective COD reduction. Likewise, the $TiO_2/UV/O_3$ processes and as depicted in Fig. 13S, the COD reduction was higher in the first 30 min of treatment, when the pH value of the WW was mainly alkaline. When the pH dropped to neutral or acidic values, the COD reduction rate tended to decrease, probably due to the reasons stated in the Section 3.1.

3.6. Comparison between technologies

When comparing the three types of AOPs ($TiO_2/UV/O_3$, $TiO_2/UV/H_2O_2$ and $TiO_2/UV/O_3/H_2O_2$) studied in this work, it is important to conclude which oxidants added to the photocatalytic process can increase the efficiency of the process. $TiO_2/UV/H_2O_2$ revealed to be the less effective process with 73% of t-VOCs degradation and 18% of COD reduction achieved in experiment 11 (Table 1: r_{ox} of 1.1; 100 mgTiO_2/L) This can be related with the lower oxidation potential of H_2O_2 comparing with O_3 and also with the fact that at alkaline medium it can be dissociated to less effective forms like perhydroxyl ions [90].

Looking to the carboxylic acids degradation, it is clear that $TiO_2/UV/H_2O_2$ was less efficient, probably due to a lower efficiency to produce reactive species in basic pH conditions. These processes produced laurylic, decanoic and nonanoic acid as by-products. The formation of carboxylic acids is an expected phenomenon, since they can be generated from the cleavage of aromatic compounds as already discussed. $HO^{\bullet}$ can be produced from the combination of UV and H_2O_2 in bulk solution and with the photoactivation of TiO_2. In the case of O_3 and O_3/H_2O_2, $HO^{\bullet}$ can also be generated from sole O_3. Under basic pH conditions, O_3 based AOPs generally produced higher amount of $HO^{\bullet}$ which led to higher reaction rate constant. These possibilities sustain

the fact that $TiO_2/UV/O_3/H_2O_2$ process obtained complete degradation of all carboxylic acids studied. $TiO_2/UV/O_3$ had an increase of decanoic and nonanoic acid concentration (18 and 17% respectively).

The most efficient process in VOCs degradation was $TiO_2/UV/O_3/H_2O_2$ in experiment 17 (Table 1: r_{ox} of 1.1; 100 mgTiO_2/L) with 86% degradation of t-VOCs and COD reduction of 43%. The optimal process was $TiO_2/UV/O_3/H_2O_2$ in experiment 13 (Table 1: r_{ox} of 0.50; 100 mgTiO_2/L) with 82% degradation of t-VOCs and a COD reduction of 38%. $TiO_2/UV/O_3/H_2O_2$ reached similar efficiency of $TiO_2/UV/O_3$ using lower amount of catalyst and oxidants.

Increasing the r_{ox} and TiO_2 concentration, the COD reduction efficiency of $TiO_2/UV/O_3$ increases. The COD reduction efficiency of $TiO_2/UV/O_3$ at higher r_{ox} and TiO_2 concentration surpassing that of $TiO_2/UV/O_3/H_2O_2$. For instance, the $TiO_2/UV/O_3$ in experiment 5 (Table 1: r_{ox} of 1.50; 500 mgTiO_2/L) achieved 55% of COD reduction, when $TiO_2/UV/O_3/H_2O_2$ in experiment 17 (Table 1: r_{ox} of 1.10; 100 mgTiO_2/L) had a COD reduction of 43%. Nevertheless, it is clear that doubling the r_{ox} value above 1 did not increased significantly the COD reduction. It means that some of the compounds or by-products of the compounds degradation were not effectively degraded under the conditions used in this work. This behavior was also reported in our previous work using industrial effluents from bitumen production [91].

The rate of degradation is also an important factor to determine the efficiency of the process, since it allows to determine the time needed to reach the milestone of degradation. This could not only helps in saving the time but also reduces the cost of the treatment in the case of faster processes. The most efficient processes of each studied AOPs was used to check which one had the best rate of degradation. A milestone setpoint of 50% was used for such a comparison. 50% degradation of O-VOCs was achieved in 30 and 15 min by using $TiO_2/UV/O_3$ and $TiO_2/UV/O_3/H_2O_2$, respectively (Tables 1S and 2S, SI). $TiO_2/UV/H_2O_2$ reached the 50% milestone only at the end of the treatment, i.e. 100 min (Tables 1S and 2S, SI). To degrade O-VOCs, the $TiO_2/UV/O_3$ in experiment 5 (Table 1: r_{ox} of 1.50; 500 mgTiO_2/L), had the highest degradation rate with 83% degradation in 15 min of treatment. In terms of VNCs, Tables 1S and 2S reveal that $TiO_2/UV/O_3/H_2O_2$ and $TiO_2/UV/O_3$ reached the 50% milestone at similar times, between 30 and 60 min, but the process with the highest degradation rate was once more experiment 5 (Table 1: r_{ox} of 1.50; 500 mgTiO_2/L) with 62% in 15 min. VSCs reached the 50% milestone in 15 min of treatment in the most efficient $TiO_2/UV/O_3$ processes and 30 min of treatment in the case of $TiO_2/UV/O_3/H_2O_2$. $TiO_2/UV/O_3$ in experiment 1 (Table 1: r_{ox} of 0.70; 100 mgTiO_2/L) had the highest degradation rate with 74% of degradation in 15 min. Regarding the carboxylic acids, it took more time to reach the 50% milestone and in some cases this level of degradation was not obtained during the time of treatment. Surprisingly, the process with the highest degradation rate for carboxylic acids was $TiO_2/UV/O_3$ experiment 6 (Table 1: r_{ox} of 0.4; 500 mgTiO_2/L) has revealed from 60% degradation in 15 min of treatment. In terms of t-VOCs, $TiO_2/UV/O_3$ processes reached this milestone faster than $TiO_2/UV/O_3/H_2O_2$ and $TiO_2/UV/H_2O_2$, needing between 15 and 30 min, while $TiO_2/UV/O_3/H_2O_2$ processes needed 30 min to reach the 50% milestone ((Tables 1S and 2S, SI). It was concluded that the most efficient process was $TiO_2/UV/O_3$ experiment 5 (Table 1: r_{ox} of 1.50; 500 mgTiO_2/L) needing only 15 min to reach 66% of the t-VOCs degradation.

It is clear that despite the fact that $TiO_2/UV/O_3/H_2O_2$ could reach similar t-VOCs degradation to $TiO_2/UV/O_3$ using a lower dose of TiO_2 and r_{ox}, it needed more time to reach certain milestones like 50%.

3.7. Process cost analysis

To evaluate the possibility of using these technologies in further studies using real industrial effluents, it is important to perform a cost analysis of each process to determine whether it is applicable in a real case scenario. Therefore, a simple cost evaluation analysis was performed for all studied processes. A similar methodology performed by Gagol and co-workers [78] was followed to determine the chemicals and energy cost. To determine the equipment costs used in this work were summed and the maintenance cost was determined as performed in our previous work [42], which in this case is approx. 3% of the main equipment cost. H_2O_2 (30% solution) had a cost of 500 American dollars ($)/ton. A TiO_2 market report from 2018 shows that the average cost of this commodity is approx. 3000$/ton [92,93]. In Poland, the price of electricity for industrial customers is around 0.11 $/kWh (3600 kJ). Furthermore, the prices of the power of the ozone generator, UV lamp and oxidant pump were also taken to account while performing the cost calculations. Ozone generator had a working power of 450 W and a price of 7600 $, the UV lamp had a power of 250 W and a cost of 189 $ per lamp with 10,000 h of live time. The oxidant pump had a working power of 80 W with a value of 2000 $. Finally, the cost of the reactor to perform the treatment, with a working volume of 15 m^3, has a cost of approx. 15,000 $. Table 4 presents the calculations to determine the treatment cost and the investment cost of each technology studied. The chemical cost is the sum of the catalyst cost (if used) and oxidant cost. It was determined first for each batch of 5 L (volume used in the experiments) and afterwards re-calculated to 1 m^3. The energy cost was determined by the same approach as the chemical cost. The operation cost is represented as American dollars per liter of treated WW ($/$m^3$). The time and dose of chemicals of each process was determined when reaching the milestone of 80% of t-VOCs degradation – only ozone and peroxone based AOPs reached this assumption.

Analyzing Table 4, the investment cost increases with the addition of the UV. Also, the O_3/H_2O_2 based processes had an investment cost higher than the O_3 processes. This is somehow expected due to the increase of the number of equipment needed. The maintenance cost followed the same trend that the equipment costs. Regarding the operational costs, Table 4 reveals that $TiO_2/UV/O_3$ processes had a cost around 15 $/$m^3$ and sole use of O_3 was slightly more expensive (17 $/$m^3$). However, the O_3/UV revealed to be the cheapest process studied in this work with 4 $/$m^3$. The catalyst did not decrease the treatment time to reach the milestone and therefore only increased significantly the process cost when comparing with O_3/UV.

The positive effect of the catalyst was observed for peroxone based AOPs - The catalyst allowed to obtain the milestone in shorter period of time comparing to non-catalytic processes. It significantly lowered the energy costs, compensating the catalyst costs. In overall $TiO_2/UV/O_3/H_2O_2$ had the same process cost as of O_3/H_2O_2/UV – 17 $/$m^3$.

Independently of the above analysis, detailed comparison of degradation results (on the basis of Table 2) reveals that there are only two processes that allow to obtain degradation of each of studied VOCs exceeding 80% (above analysis was performed for milestone referring to total content of VOCs). The compounds that are limiting the application of the cheapest AOPs from the comparison (i.e. the O_3/UV process with treatment cost of 4$/$m^3$) are naphthalene, 2-nitro-phenol and 2-nitro-toluene. These compounds revealed to be persistent to degradation in O_3/UV system. In this cases application of photocatalytic treatment based on TiO_2 is a must. In this case the process cost will be higher – 15,42$/$m^3$ and treatment technology will be based on $TiO_2/UV/O_3$.

4. Conclusions

The studies performed in this work aimed the evaluation of the efficiency of photolytic (UV) and photocatalytic (UV/TiO_2) processes based on three different classical oxidants, O_3, H_2O_2 and O_3/H_2O_2, on a model WW with variety of VOCs. The sole use of oxidants studied, re-

vealed that O_3/H_2O_2 obtain the highest efficiency with 92% of t-VOCs degradation and a COD reduction of 46%. The combination of UV with O_3 and H_2O_2 increased the degradation efficiency compared to sole H_2O_2 and O_3. The addition of TiO_2 to the UV based technologies proved to induce a further increase in the treatment efficiency in all three types of technologies used.

The present study revealed that $TiO_2/UV/O_3$ and $TiO_2/UV/O_3/H_2O_2$ are efficient technologies to degrade several types of VOCs in a relatively short time and using small amount of chemicals.

This studies revealed, that for most types of organic pollutants a systems based on UV/O_3 are providing satisfactory results with low cost of treatment cost – a 4 $/m^3. In terms of nitrogen-containing VOCs, application of photocatalytic system based on TiO_2 is obligatory to obtain high degree of degradation. In this case the cost of treatment is increases to approx. 15 $/m^3. Presented solutions were tested in large laboratory scale reactor, possible to routine scale-up to process scale, making these achievements available to industrial application.

Acknowledgment

The authors gratefully acknowledge the financial support from the National Science Centre, Warsaw, Poland – decision no. DEC-2013/09/D/ST8/03973 and UMO-2017/25/B/ST8/01364.

The authors gratefully acknowledge the Evonik Industries for kindly providing the AEROXIDE® TiO2 P 25 Titanium dioxide.

Appendix A. Supplementary material

Supplementary data to this article can be found online at https://doi.org/10.1016/j.seppur.2019.05.012.

References

[1] Y. Xie, L. Chen, R. Liu, Oxidation of AOX and organic compounds in pharmaceutical wastewater in RSM-optimized-Fenton system, Chemosphere 155 (2016) 217–224, https://doi.org/10.1016/j.chemosphere.2016.04.057.

[2] A.S. Costa, L.P.C. Romão, B.R. Araújo, S.C.O. Lucas, S.T.A. Maciel, A. Wisniewski, M.R. Alexandre, Environmental strategies to remove volatile aromatic fractions (BTEX) from petroleum industry wastewater using biomass, Bioresour. Technol. 105 (2012) 31–39, https://doi.org/10.1016/j.biortech.2011.11.096.

[3] P. Stepnowski, E.M. Siedlecka, P. Behrend, B. Jastorff, Enhanced photo-degradation of contaminants in petroleum refinery wastewater, Water Res. 36 (2002) 2167–2172.

[4] A. Latorre, A. Rigol, S. Lacorte, D. Barcelo, C omparison of gas chromatography – mass spectrometry and liquid chromatography – mass spectrometry for the determination of fatty and resin acids in paper mill process waters, J. Chromatogr. A 991 (2003) 205–215, https://doi.org/10.1016/S0021-9673(03)00217-6.

[5] A. Rigol, A. Latorre, S. Lacorte, D. Barceló, Determination of toxic compounds in paper-recycling process waters by gas chromatography-mass spectrometry and liquid chromatography-mass spectrometry, J. Chromatogr. A 963 (2002) 265–275, https://doi.org/10.1016/S0021-9673(02)00232-7.

[6] X.A. Ning, J.Y. Wang, R.J. Li, W. Bin Wen, C.M. Chen, Y.J. Wang, Z.Y. Yang, J.Y. Liu, Fate of volatile aromatic hydrocarbons in the wastewater from six textile dyeing wastewater treatment plants, Chemosphere 136 (2015) 50–55, https://doi.org/10.1016/j.chemosphere.2015.03.086.

[7] M. Castillo, Characterization of organic pollutants in industrial effluents by high-temperature gas chromatography–mass spectrometry, TrAC Trends Anal. Chem. 18 (1999) 26–36, https://doi.org/10.1016/S0165-9936(98)00066-1.

[8] L.B. Paulik, C.E. Donald, B.W. Smith, L.G. Tidwell, K.A. Hobbie, L. Kincl, E.N. Haynes, K.A. Anderson, Emissions of polycyclic aromatic hydrocarbons from natural gas extraction into air, Environ. Sci. Technol. 50 (2016) 7921–7929, https://doi.org/10.1021/acs.est.6b02762.

[9] A.T. Nielsen, S. Jonsson, Quantification of volatile sulfur compounds in complex gaseous matrices by solid-phase microextraction, J. Chromatogr. A. 963 (2002) 57–64, https://doi.org/10.1016/S0021-9673(02)00556-3.

[10] F. Lestremau, V. Desauziers, J.C. Roux, J.L. Fanlo, Development of a quantification method for the analysis of malodorous sulphur compounds in gaseous industrial effluents by solid-phase microextraction and gas chromatography-pulsed flame photometric detection, J. Chromatogr. A 999 (2003) 71–80, https://doi.org/10.1016/S0021-9673(03)00328-5.

[11] G. Boczkaj, A. Fernandes, P. Makoś, Study of different advanced oxidation processes for wastewater treatment from petroleum bitumen production at basic pH, Ind. Eng. Chem. Res. 56 (2017) 8806–8814, https://doi.org/10.1021/acs.iecr.7b01507.

[12] A. Fernandes, P. Makos, G. Boczkaj, Treatment of bitumen post oxidative effluents by sulfate radicals based advanced oxidation processes (S-AOPs) under alkaline pH conditions, J. Clean. Prod. 195 (2018) 374–384, https://doi.org/10.1016/j.jclepro.2018.05.207.

[13] M. Pimentel, N. Oturan, M. Dezotti, M.A. Oturan, Phenol degradation by advanced electrochemical oxidation process electro-Fenton using a carbon felt cathode, Appl. Catal. B Environ. 83 (2008) 140–149, https://doi.org/10.1016/j.apcatb.2008.02.011.

[14] S. Popiel, T. Nalepa, D. Dzierzak, R. Stankiewicz, Z. Witkiewicz, Rate of dibutylsulfide decomposition by ozonation and the O3/H2O2 advanced oxidation process, J. Hazard. Mater. 164 (2009) 1364–1371, https://doi.org/10.1016/j.jhazmat.2008.09.049.

[15] Y. Chu, D. Zhang, L. Liu, Y. Qian, L. Li, Electrochemical degradation of m-cresol using porous carbon-nanotube-containing cathode and Ti/SnO2-Sb2O5-IrO2anode: Kinetics, byproducts and biodegradability, J. Hazard. Mater. 252–253 (2013) 306–312, https://doi.org/10.1016/j.jhazmat.2013.03.018.

[16] A. Long, Y. Lei, H. Zhang, Degradation of toluene by a selective ferrous ion activated persulfate oxidation process, Ind. Eng. Chem. Res. 53 (2014) 1033–1039, https://doi.org/10.1021/ie402633n.

[17] J. Kazumi, M.E. Caldwell, J.M. Suflita, D.R. Lovley, L.Y. Young, Anaerobic degradation of benzene in diverse environments, Environ. Sci. Technol. 31 (1997) 813–818, https://doi.org/10.1021/es960506a.

[18] C. Liang, Y.Y. Guo, Mass transfer and chemical oxidation of naphthalene particles with zerovalent iron activated persulfate, Environ. Sci. Technol. 44 (2010) 8203–8208, https://doi.org/10.1021/es903411a.

[19] P.S. Majumder, S.K. Gupta, Hybrid reactor for priority pollutant nitrobenzene removal, Water Res. 37 (2003) 4331–4336, https://doi.org/10.1016/S0043-1354(03)00436-6.

[20] S.I. Mulla, R.S. Hoskeri, Y.S. Shouche, H.Z. Ninnekar, Biodegradation of 2-Nitrotoluene by Micrococcus sp. strain SMN-1, Biodegradation 22 (2011) 95–102, https://doi.org/10.1007/s10532-010-9379-3.

[21] W.H. Glaze, J. Kangt, Advanced oxidation processes. Test of a kinetic model for the oxidation of organic compounds with ozone and hydrogen peroxide in a semibatch reactor, Ind. Eng. Chem. Res. 28 (1989) 1580–1587, https://doi.org/10.1021/ie00095a002.

[22] M. Litter, Introduction to photochemical advanced oxidation processes for water treatment, in: P. Boule, D.W. Bahnemann, P.K.J. Robertson (Eds.), Environ. Photochem. Part II, Springer Berlin Heidelberg, 2005, pp. 325–366, https://doi.org/10.1007/b89482.

[23] D. Shahidi, R. Roy, A. Azzouz, Advances in catalytic oxidation of organic pollutants – prospects for thorough mineralization by natural clay catalysts, Appl. Catal. B Environ. 174–175 (2015) 277–292, https://doi.org/10.1016/j.apcatb.2015.02.042.

[24] N.S. Shah, J.A. Khan, M. Sayed, Z.U.H. Khan, H.S. Ali, B. Murtaza, H.M. Khan, M. Imran, N. Muhammad, Hydroxyl and sulfate radical mediated degradation of ciprofloxacin using nano zerovalent manganese catalyzed S2O8 2–, Chem. Eng. J. 356 (2019) 199–209, https://doi.org/10.1016/j.cej.2018.09.009.

[25] J.M. Poyatos, M.M. Muñio, M.C. Almecija, J.C. Torres, E. Hontoria, F. Osorio, Advanced oxidation processes for wastewater treatment: state of the art, Water. Air. Soil Pollut. 205 (2010) 187–204, https://doi.org/10.1007/s11270-009-0065-1.

[26] M. Sayed, M. Gul, N.S. Shah, J.A. Khan, Z. Ul, H. Khan, F. Rehman, A.R. Khan, S. Rauf, H. Arandiyan, C.P. Yang, In-situ dual applications of ionic liquid coated Co2+ and Fe3+ co-doped TiO2: superior photocatalytic degradation of ofloxacin at pilot scale level and enhanced peroxidase like activity for calorimetric biosensing, J. Mol. Liq. 282 (2019) 275–285, https://doi.org/10.1016/j.molliq.2019.03.022.

[27] M. Sayed, A. Arooj, N.S. Shah, J.A. Khan, L.A. Shah, F. Rehman, H. Arandiyan, A.M. Khan, A.R. Khan, Narrowing the band gap of TiO2 by co-doping with Mn2+ and Co2+ for efficient photocatalytic degradation of enoxacin and its additional peroxidase like activity: a mechanistic approach, J. Mol. Liq. 272 (2018) 403–412, https://doi.org/10.1016/j.molliq.2018.09.102.

[28] N.S. Shah, J.A. Khan, M. Sayed, Z.U.H. Khan, A.D. Rizwan, N. Muhammad, G. Boczkaj, B. Murtaza, M. Imran, H.M. Khan, G. Zaman, Solar light driven degradation of norfloxacin using as-synthesized Bi3+and Fe2+co-doped ZnO with the addition of HSO5−: toxicities and degradation pathways investigation, Chem. Eng. J. 351 (2018) 841–855, https://doi.org/10.1016/j.cej.2018.06.111.

[29] Z.S. Seddigi, A. Bumajdad, S.P. Ansari, S.a. Ahmed, E.Y. Danish, N.H. Yarkandi, S. Ahmed, Preparation and characterization of Pd doped ceria-ZnO nanocomposite catalyst for methyl tert-butyl ether (MTBE) photodegradation, J. Hazard. Mater. 264 (2014) 71–78, https://doi.org/10.1016/j.jhazmat.2013.10.070.

[30] B. Murtaza, N.S. Shah, M. Sayed, J. Ali, M. Imran, M. Shahid, Z. Ul, H. Khan, A. Ghani, G. Murtaza, N. Muhammad, M. Sha, N. Khan, Synergistic effects ofbismuth coupling on the reactivity and reusability of zerovalent iron nanoparticles for the removal of cadmium from aqueous solution, Sci. Total Environ. 669 (2019) 333–341, https://doi.org/10.1016/j.scitotenv.2019.03.062.

[31] F.H. Margha, M.S. Abdel-Wahed, T.A. Gad-Allah, Nanocrystalline Bi2O3–B2O3–(MoO3 or V2O5) glass-ceramic systems for organic pollutants degradation, Ceram. Int. 41 (2015) 5670–5676, https://doi.org/10.1016/j.ceramint.2014.12.152.

[32] R. Darvishi, C. Soltani, M. Mashayekhi, M. Naderi, G. Boczkaj, S. Jorfi, M. Safari, Sonocatalytic degradation of tetracycline antibiotic using zinc oxide nanostructures loaded on nano-cellulose from waste straw as nanosonocatalyst, Ultrason. – Sonochem. 55 (2019) 117–124, https://doi.org/10.1016/j.ultsonch.2019.03.009.

[33] R. Mirzaee, R. Darvishi, C. Soltani, A. Khataee, G. Boczkaj, Combination of air-dispersion cathode with sacrificial iron anode generating Fe2+Fe3+2O4 nanostruc-

tures to degrade paracetamol under ultrasonic irradiation, J. Mol. Liq. 284 (2019) 536–546, https://doi.org/10.1016/j.molliq.2019.04.033.
[34] S.-Y. Lee, S.-J. Park, TiO2 photocatalyst for water treatment applications, J. Ind. Eng. Chem. 19 (2013) 1761–1769, https://doi.org/10.1016/j.jiec.2013.07.012.
[35] K.H. Kim, S.K. Ihm, Heterogeneous catalytic wet air oxidation of refractory organic pollutants in industrial wastewaters: a review, J. Hazard. Mater. 186 (2011) 16–34, https://doi.org/10.1016/j.jhazmat.2010.11.011.
[36] L.F. Liotta, M. Gruttadauria, G. Di Carlo, G. Perrini, V. Librando, Heterogeneous catalytic degradation of phenolic substrates: catalysts activity, J. Hazard. Mater. 162 (2009) 588–606, https://doi.org/10.1016/j.jhazmat.2008.05.115.
[37] K.M. Lee, C.W. Lai, K.S. Ngai, J.C. Juan, Recent developments of zinc oxide based photocatalyst in water treatment technology: a review, Water Res. 88 (2016) 428–448, https://doi.org/10.1016/j.watres.2015.09.045.
[38] A.L. Mota, L.F. Albuquerque, L.C. Beltrame, O. Chiavone-Filho, A. Machulek Jr, C.A. Nascimento, Advanced oxidation processes and their application in the petroleum industry: a review, Brazilian J. Pet. Gas. 2 (2009) 122–142 http://www.portalabpg.org.br/bjpg/index.php/bjpg/article/view/57.
[39] A.R. Ribeiro, O.C. Nunes, M.F.R. Pereira, A.M.T. Silva, An overview on the advanced oxidation processes applied for the treatment of water pollutants defined in the recently launched Directive 2013/39/EU, Environ. Int. 75 (2015) 33–51, https://doi.org/10.1016/j.envint.2014.10.027.
[40] T.A. Kurniawan, L. Yanyan, T. Ouyang, A.B. Albadarin, G. Walker, BaTiO 3 /TiO 2 composite-assisted photocatalytic degradation for removal of acetaminophen from synthetic wastewater under UV–vis irradiation, Mater. Sci. Semicond. Process. 73 (2018) 42–50, https://doi.org/10.1016/j.mssp.2017.06.048.
[41] M. Tammaro, V. Fiandra, M.C. Mascolo, A. Salluzzo, C. Riccio, A. Lancia, Photocatalytic degradation of atenolol in aqueous suspension of new recyclable catalysts based on titanium dioxide, J. Environ. Chem. Eng. 5 (2017) 3224–3234, https://doi.org/10.1016/j.jece.2017.06.026.
[42] G. Boczkaj, A. Fernandes, Wastewater treatment by means of Advanced Oxidation Processes at basic pH conditions: a review, Chem. Eng. J. 320 (2017) 608–633, https://doi.org/10.1016/j.cej.2017.03.084.
[43] M. Goel, H. Hongqiang, A.S. Mujumdar, M.B. Ray, Sonochemical decomposition of volatile and non-volatile organic compounds – a comparative study, Water Res. 38 (2004) 4247–4261, https://doi.org/10.1016/j.watres.2004.08.008.
[44] S.B. Kim, S.C. Hong, Kinetic study for photocatalytic degradation of volatile organic compounds in air using thin film TiO2 photocatalyst, Appl. Catal. B Environ. 35 (2002) 305–315, https://doi.org/10.1016/S0926-3373(01)00274-0.
[45] H.-H. Cheng, C.-C. Hsieh, Removal of aromatic volatile organic compounds in the sequencing batch reactor of petroleum refinery wastewater treatment plant, CLEAN – Soil, Air, Water. 41 (2013) 765–772, https://doi.org/10.1002/clen.201100112.
[46] Y.-S. Shen, Y. Ku, Treatment of gas-phase volatile organic compounds (VOCs) by the process, Chemosphere 38 (1999) 1855–1866, https://doi.org/10.1016/S0045-6535(98)00400-7.
[47] R.M. Alberici, W.F. Jardim, Photocatalytic destruction of VOCS in the gas-phase using titanium dioxide, Appl. Catal. B Environ. 14 (1997) 55–68, https://doi.org/10.1016/S0926-3373(97)00012-X.
[48] A. Fernandes, P. Makoś, J.A. Khan, G. Boczkaj, Pilot scale degradation study of 16 selected volatile organic compounds by hydroxyl and sulfate radical based advanced oxidation processes, J. Clean. Prod. 208 (2019) 54–64, https://doi.org/10.1016/j.jclepro.2018.10.081.
[49] G. Boczkaj, P. Makoś, A. Przyjazny, Application of dispersive liquid-liquid microextraction and gas chromatography-mass spectrometry (DLLME-GC-MS) for the determination of oxygenated volatile organic compounds in effluents from the production of petroleum bitumen, J. Sep. Sci. 39 (2016) 2604–2615.
[50] P. Makoś, A. Fernandes, G. Boczkaj, Method for the simultaneous determination of monoaromatic and polycyclic aromatic hydrocarbons in industrial effluents using dispersive liquid-liquid microextraction with GC-MS, J. Sep. Sci. (2018) 1–25, https://doi.org/10.1002/jssc.201701464.
[51] P. Makoś, A. Fernandes, A. Przyjazny, G. Boczkaj, Sample preparation procedure using extraction and derivatization of carboxylic acids from aqueous samples by means of deep eutectic solvents for gas chromatographic-mass spectrometric analysis, J. Chromatogr. A 1555 (2018) 10–19, https://doi.org/10.1016/j.chroma.2018.04.054.
[52] R. Alnaizy, A. Akgerman, Advanced oxidation of phenolic compounds, Adv. Environ. Res. 4 (2000) 233–244, https://doi.org/10.1016/S1093-0191(00)00024-1.
[53] L. Zhao, J. Ma, Z.zhong. Sun, Oxidation products and pathway of ceramic honeycomb-catalyzed ozonation for the degradation of nitrobenzene in aqueous solution, Appl. Catal. B Environ. 79 (2008) 244–253, https://doi.org/10.1016/j.apcatb.2007.10.026.
[54] B. Pal, T. Hata, K. Goto, G. Nogami, Photocatalytic degradation of o-cresol sensitized by iron-titania binary photocatalysts, J. Mol. Catal. A: Chem. 169 (2001) 147–155, https://doi.org/10.1016/S1381-1169(00)00549-5.
[55] S. Hisaindee, M.A. Meetani, M.A. Rauf, Application of LC-MS to the analysis of advanced oxidation process (AOP) degradation of dye products and reaction mechanisms, TrAC – Trends Anal. Chem. 49 (2013) 31–44, https://doi.org/10.1016/j.trac.2013.03.011.
[56] J. Fenoll, M. Martínez-Menchón, G. Navarro, N. Vela, S. Navarro, Photocatalytic degradation of substituted phenylurea herbicides in aqueous semiconductor suspensions exposed to solar energy, Chemosphere 91 (2013) 571–578, https://doi.org/10.1016/j.chemosphere.2012.11.067.
[57] M. Cristina Yeber, J. Rodríguez, J. Freer, N. Durán, H.D. Mansilla, Photocatalytic degradation of cellulose bleaching effluent by supported TiO2 and ZnO, Chemosphere 41 (2000) 1193–1197, https://doi.org/10.1016/S0045-6535(99)00551-2.
[58] U.I. Gaya, A.H. Abdullah, M.Z. Hussein, Z. Zainal, Photocatalytic removal of 2,4,6-trichlorophenol from water exploiting commercial ZnO powder, Desalination 263 (2010) 176–182, https://doi.org/10.1016/j.desal.2010.06.055.
[59] Z. Zhou, P. Zhang, Y. Lin, E. Ashalley, H. Ji, J. Wu, H. Li, Z. Wang, Microwave fabrication of Cu2ZnSnS4nanoparticle and its visible light photocatalytic properties, Nanoscale Res. Lett. 9 (2014) 1–6, https://doi.org/10.1186/1556-276X-9-477.
[60] E. Ra, Advances in photo-catalytic materials for environmental applications, J. Mater. Sci. 4 (2016) 26–50.
[61] H. Zangeneh, a.a.L. Zinatizadeh, M. Feizy, A comparative study on the performance of different advanced oxidation processes (UV/O3/H2O2) treating linear alkyl benzene (LAB) production plant's wastewater, J. Ind. Eng. Chem. 20 (2014) 1453–1461, https://doi.org/10.1016/j.jiec.2013.07.031.
[62] O. Gimeno, F.J. Rivas, F.J. Beltrán, M. Carbajo, Photocatalytic ozonation of winery wastewaters, J. Agric. Food Chem. 55 (2007) 9944–9950, https://doi.org/10.1021/jf072167i.
[63] M. Novak, G.M. Loudon, The pKa of acetophenone in aqueous solution, J. Org. Chem. 42 (1977) 2494–2498, https://doi.org/10.1021/jo00434a032.
[64] (2017) Engineering ToolBox, Phenols, alcohols and carboxylic acids – pKa values., n.d. https://www.engineeringtoolbox.com/paraffinic-benzoic-hydroxy-dioic-acids-structure-pka-carboxylic-dissociation-constant-alcohol-phenol-d_1948.html (accessed August 17, 2018).
[65] (2017) Engineering ToolBox, Amines, diamines and cyclic organic nitrogen compounds – pKa values, n.d. https://www.engineeringtoolbox.com/amine-diamine-pyridine-cyclic-quinoline-aminobenzene-structure-pka-carboxylic-dissociation-constant-d_1949.html (accessed August 17, 2018).
[66] J.A. Navio, M. Garcia Gómez, M.A. Pradera Adrian, J. Fuentes Mota, Partial or complete heterogeneous photocatalytic oxidation of neat toluene and 4-picoline in liquid organic oxygenated dispersions containing pure or iron-doped titania photocatalysts, J. Mol. Catal. A: Chem. 104 (1996) 329–339, https://doi.org/10.1016/1381-1169(95)00155-7.
[67] C.K. Chua, M. Pumera, Influence of methyl substituent position on redox properties of nitroaromatics related to 2,4,6-trinitrotoluene, Electroanalysis 23 (2011) 2350–2356, https://doi.org/10.1002/elan.201100359.
[68] A.S. Borovik, S.G. Bott, A.R. Barron, Hydrogen/deuterium exchange catalyzed by an unusually stable mercury ± toluene complex, Angew. Chem. Int. Ed. Engl. 39 (2000) 4117–4118.
[69] K.H. Wang, Y.H. Hsieh, M.Y. Chou, C.Y. Chang, Photocatalytic degradation of 2-chloro and 2-nitrophenol by titanium dioxide suspensions in aqueous solution, Appl. Catal. B Environ. 21 (1999) 1–8, https://doi.org/10.1016/S0926-3373(98)00116-7.
[70] G.W. Wheland, J. Farr, Acid strengths of aliphatic nitro compounds, J. Am. Chem. Soc. 65 (1943), 1433-1433.
[71] C.B. Menon, E. Buncel, Hydrogenolysis of organometallics and the acidity of hydrogen, Can. J. Chem. 54 (1976) 3949–3954.
[72] J.R. Baker, M.W. Milke, J.R. Mihelcic, Relationship between chemical and theoretical oxygen demand for specific classes of organic chemicals, Water Res. 33 (1999) 327–334, https://doi.org/10.1016/S0043-1354(98)00231-0.
[73] M.O. Buffle, U. Von Gunten, Phenols and amine induced HO• generation during the initial phase of natural water ozonation, Environ. Sci. Technol. 40 (2006) 3057–3063, https://doi.org/10.1021/es052020c.
[74] S. Soltan, H. Jafari, S. Afshar, O. Zabihi, Enhancement of photocatalytic degradation of furfural and acetophenone in water media using nano-TiO2-SiO2 deposited on cementitious materials, Water Sci. Technol. 74 (2016) 1689–1697, https://doi.org/10.2166/wst.2016.343.
[75] K. Okamoto, Y. Yamamoto, H. Tanaka, M. Tanaka, A. Itaya, Heterogeneous photocatalytic decomposition of phenol over TiO2 powder, Bull. Chem. Soc. Jpn. 58 (1985) 2015–2022, https://doi.org/10.1246/bcsj.58.2015.
[76] E.R.L. Tiburtius, P. Peralta-Zamora, A. Emmel, Treatment of gasoline-contaminated waters by advanced oxidation processes, J. Hazard. Mater. 126 (2005) 86–90, https://doi.org/10.1016/j.jhazmat.2005.06.003.
[77] G. Boczkaj, M. Gągol, M. Klein, A. Przyjazny, Effective method of treatment of effluents from production of bitumens under basic pH conditions using hydrodynamic cavitation aided by external oxidants, Ultrason. Sonochem. 40 (2018) 969–979, https://doi.org/10.1016/j.ultsonch.2017.08.032.
[78] M. Gągol, A. Przyjazny, G. Boczkaj, Highly effective degradation of selected groups of organic compounds by cavitation based AOPs under basic pH conditions, Ultrason. Sonochem. 45 (2018) 257–266, https://doi.org/10.1016/j.ultsonch.2018.03.013.
[79] M. Gagol, A. Przyjazny, G. Boczkaj, Wastewater treatment by means of advanced oxidation processes based on cavitation – a review, Chem. Eng. J. 338 (2018) 599–627, https://doi.org/10.1016/j.cej.2018.01.049.
[80] D. Vione, V. Maurino, C. Minero, M. Lucchiari, Nitration and hydroxylation of benzene in the presence of nitrite/nitrous acid in aqueous solution, Chemosphere 56 (2004) 1049–1059, https://doi.org/10.1016/j.chemosphere.2004.05.027.
[81] D. Borghesi, D. Vione, V. Maurino, C. Minero, Transformations of benzene photoinduced by nitrate salts and iron oxide, J. Atmos. Chem. 52 (2005) 259–281, https://doi.org/10.1007/s10874-005-5304-2.
[82] D. Vione, V. Maurino, C. Minero, E. Pelizzetti, Phenol photonitration upon UV irradiation of nitrite in aqueous solution I: Effects of oxygen and 2-propanol, Chemosphere 45 (2001) 893–902, https://doi.org/10.1016/S0045-6535(01)00035-2.

[83] A.E. Gekhman, I.P. Stolyarov, A.F. Shestakov, A.E. Shilov, I.I. Moiseev, Oxidation of molecular nitrogen with hydrogen peroxide, Russ. Chem. Bull. Int.Ed. 52 (2003) 768–770.
[84] R. Ameta, A. Kumar, P.B. Punjabi, S.C. Ameta, Advanced oxidation processes: basics and principles, in: D.G. Rao, R. Senthilkumar, J. Anthony Byrne (Eds.), Wastewater Treat. Adv. Process. Technol., 2013th ed., CRC Press and IWA Publishing, USA, 2013, pp. 61–107, https://doi.org/10.1007/s13398-014-0173-7.2.
[85] Z. Chen, X. Yu, X. Huang, S. Zhang, Prediction of reaction rate constants of hydroxyl radical with organic compounds, J. Chil. Chem. Soc. 59 (2014) 2252–2259, https://doi.org/10.4067/S0717-97072014000100003.
[86] H. Suzuki, S. Araki, H. Yamamoto, Evaluation of advanced oxidation processes (AOP) using O3, UV, and TiO2 for the degradation of phenol in water, J. Water Process Eng. 7 (2015) 54–60, https://doi.org/10.1016/j.jwpe.2015.04.011.
[87] M.H.M.T. Assumpção, R.F.B. De Souza, R.M. Reis, R.S. Rocha, J.R. Steter, P. Hammer, I. Gaubeur, M.L. Calegaro, M.R.V. Lanza, M.C. Santos, Low tungsten content of nanostructured material supported on carbon for the degradation of phenol, Appl. Catal. B Environ. 142–143 (2013) 479–486, https://doi.org/10.1016/j.apcatb.2013.05.024.
[88] V.S. Mohite, M.A. Mahadik, S.S. Kumbhar, Y.M. Hunge, J.H. Kim, A.V. Moholkar, K.Y. Rajpure, C.H. Bhosale, Photoelectrocatalytic degradation of benzoic acid using Au doped TiO2thin films, J. Photochem. Photobiol. B Biol. 142 (2015) 204–211, https://doi.org/10.1016/j.jphotobiol.2014.12.004.
[89] B. Roig, C. Gonzalez, O. Thomas, Monitoring of phenol photodegradation by ultra v iolet spectroscopy, Spectrochim. Acta Part A Mol. Biomol. Spectrosc. 59 (2003) 303–307.
[90] O. Spalek, J. Balej, I. Paseka, Kinetics of the decomposition of hydrogen peroxide in alkaline solutions, J. Chem. Soc. Faraday Trans. 78 (1982) 2349, https://doi.org/10.1039/f19827802349.
[91] G. Boczkaj, A. Fernandes, M. Gągol, Studies on treatment of bitumen effluents by means of advanced oxidation processes (AOPs) in basic pH conditions, in: G. Mannina (Ed.), Front. Wastewater Treat. Model. FICWTM 2017. Lect. Notes Civ. Eng., Springer, 2017, pp. 331–336, https://doi.org/10.1007/978-3-319-58421-8.
[92] P.P. EUWID, Upward spiral in titanium dioxide prices slowing in second quarter, EUWID Pulp Pap. 20/2018, 2018. https://www.euwid-paper.com/news/singlenews/Artikel/upward-spiral-in-titanium-dioxide-prices-slowing-in-second-quarter.html (accessed November 21, 2018).
[93] P.P. EUWID, Titanium dioxide prices left untouched in Q3, EUWID Pulp Pap. 34/2018, 2018. 3. https://www.euwid-paper.com/news/singlenews/Artikel/titanium-dioxide-prices-left- untouched-in-q3.html (accessed November 21, 2018).